2-57-62-2 • NOVEMBER 1962

TECHNICAL REPORT

THE SPECTRAL ABSORPTION COEFFICIENT OF HEATED AIR

DASA Report Control No. 1348

2-57-62-2 • NOVEMBER 1962

2-57-62-2

TECHNICAL REPORT

THE SPECTRAL ABSORPTION COEFFICIENT OF HEATED AIR

by

D. R. CHURCHILL
S. A. HAGSTROM
J. D. WEISNER
and
B. N. ARMSTRONG

DASA Report Control No. 1348

WORK CARRIED OUT UNDER DASA CONTRACT NO. DA49-166-XZ-009

Lockheed

MISSILES & SPACE COMPANY

A GROUP DIVISION OF LOCKHEED AIRCRAFT CORPORATION

SUNNYVALE, CALIFORNIA

FOREWORD

This research was supported by DASA under Contract No. DA 49-146-XZ-009. The work described in this report was performed by members of the Physical Sciences Laboratory of Lockheed Missiles & Space Company at Palo Alto, California, under the direction of Dr. R. K. M. Landshoff. Dr. S. A. Hagstrom (now at the University of Indiana) carried out the initial research and machine programs for this project, which is being continued by D. R. Churchill. Appendix B was prepared by R. W. Hille

ABSTRACT

That portion of the line absorption coefficient for heated air which depends only on the molecular band systems, i.e., not on population numbers, has been calculated for each line in the frequency region of interest, with a total of over 150,000 lines tabulated on magnetic tape.

With the results for the O_2 Schumann-Runge system, a preliminary transport calculation has been completed for a slab of molecular oxygen. The effect of line widths on transmission is illustrated, and average transmissions are given as a function of frequency. The present results are compared with those of a previous calculation.

CONTENTS

Section		Page
	FOREWORD	iii
	ABSTRACT	v
	ILLUSTRATIONS	ix
1	INTRODUCTION	1-1
2	RADIATION TRANSPORT	2-1
	2.1 The Equation of Radiation Transfer	2-1
	2.2 The Planck and Rosseland Mean Absorption Coefficients	2-2
	2.3 Importance of Line Widths in Radiation Transport	2-5
3	LINE ABSORPTION COEFFICIENT OF HEATED AIR	3-1
	3.1 Expression for the Absorption Coefficient of a Single Line	3-1
	3.2 Overlapping and Composite Lines	3-7
4	THE LINE FREQUENCIES AND LINE INTENSITIES FOR AIR	4-1
	4.1 Spectroscopic Quantum Numbers	4-1
	4.2 Symmetry Properties of the Eigenfunctions	4-2
	4.3 Coupling of the Angular Momenta	4-6
	4.4 Selection Rules and Branches	4-9
	4.5 Intensity Factors	4-11
	4.6 The $B\ ^3\Sigma_u^- - X\ ^3\Sigma_g^-$ (Schumann-Runge) System of O_2	4-12
	4.7 The $B\ ^3\Pi - A\ ^3\Sigma_u^+$ (First Positive) System of N_2	4-14
	4.8 The $N_2\ C\ ^3\Pi_u - B\ ^3\Pi_g$ (Second Positive) System	4-17
	4.9 The $B\ ^2\Sigma_u^+ - X\ ^2\Sigma_g^+$ (First Negative) System of N_2^+	4-22
	4.10 The $B\ ^2\Pi - X\ ^2\Pi$ (Beta) System of NO	4-24
	4.11 The $A\ ^2\Sigma - X\ ^2\Pi$ (Gamma) System of NO	4-28
5	THE SACHA CODES	5-1
	5.1 Magnetic-Tape Line Atlases	5-1
	5.2 Average Transmission Calculation	5-2
	5.3 Comparison of Results	5-3
	5.4 A Calculation for Heated Air	5-9
6	REFERENCES	6-1

Appendix		Page
A	TABLES	A-1
B	SUPPLEMENTARY NUCLEAR WEAPON EFFECTS STUDY	B-1

ILLUSTRATIONS

Figure		Page
4-1	Hund's Case "a"	4-7
4-2	Hund's Case "b"	4-7
4-3	$B\ ^3\Sigma_u^- - X\ ^3\Sigma_g^-$ Band of O_2 (Schumann-Runge System)	4-13
4-4	$B\ ^3\Pi_g - A\ ^3\Sigma_u^+$ Band of N_2 (1st Positive System)	4-15
4-5	$C\ ^3\Pi_u - B\ ^3\Pi_g$ Band of N_2 (2nd Positive System)	4-18
4-6	$B\ ^2\Sigma_u^+ - X\ ^2\Sigma_g^+$ Band of N_2^+ (1st Negative System)	4-23
4-7	$B\ ^2\Pi - X\ ^2\Pi$ Band of NO (β System)	4-25
4-8	$A\ ^2\Sigma - X\ ^2\Sigma$ Band of NO (γ System)	4-29
5-1	Effect of Half-Width Variation on Optical Properties of O_2 for ν = 31500 cm^{-1} and T = 2000° K	5-4
5-2	Effect of Half-Width Variation on Optical Properties of O_2 for O_2 for = 47500 cm^{-1} and T = 2000° K	5-5
5-3	SACHA Code Average Transmission Result for O_2 (σ = 0.75)	5-6
5-4	SACHA Code Average Transmission Results for O_2 (σ = 1.0)	5-7
5-5	SACHA Code Average Transmission Results for O_2 (σ = 2.0)	5-8
5-6	Average Transmission Through 1 cm of O_2 (calculated from results of Meyerott, Sokoloff, and Nicholls, 1959). Electronic f-number and populations normalized to agree with SACHA results	5-10

Section 1
INTRODUCTION

This report summarizes recent progress made toward the theoretical determination of the spectral absorption coefficient for heated air in the temperature-density region where discrete molecular transitions are dominant. Previous investigations at this laboratory have been made along similar or related lines, but the molecular spectra were not considered in such detail. Meyerott, Sokoloff, and Nicholls (Ref. 1) have calculated the spectral contribution to the absorption coefficient of air for the optically thin case, while Armstrong et al. have treated the similar atomic problem (Ref. 2). The regions in the temperature-density plane where molecular phenomena might be expected to make a sizeable contribution are pointed out in a recent article by Armstrong, Sokoloff, Nicholls, Holland, and Meyerott (Ref. 3).

In the present study, six molecular systems will be considered: the Schumann-Runge system of O_2, the first and second positive systems of N_2, the first negative system of N_2^+, and the beta and gamma systems of NO (nitric oxide). Future calculations will probably include any continuum as well as O^- photo-detachment. Other effects may be considered as the temperature-density region is extended toward that of atomic phenomena.

After necessary preliminaries are developed in Section 2, the spectral absorption coefficient is introduced in its general form (for molecular transitions) in Section 3. Section 4, after a review of spectroscopic notation, specializes the expressions of Section 3 to the six systems of interest here. Machine calculations and results are then summarized in Section 5, in which a preliminary transport code is also discussed.

Section 2

RADIATION TRANSPORT

2.1 THE EQUATION OF RADIATION TRANSFER

Each volume element in a mass of high temperature gas is simultaneously emitting and absorbing radiation of all frequencies. It is the balance between these processes which determines the local radiation flux within the gas as well as the flux which escapes. Let the flux of radiation per unit frequency interval about ν, per unit solid angle in the direction $\vec{\Omega}$ and per unit area normal to the direction $\vec{\Omega}$, be denoted by $I_\nu(\vec{\Omega})$. Similarly, denote the energy radiated by a unit mass of gas per unit frequency per unit solid angle by $j_\nu(\vec{\Omega})$. If the absorption coefficient of the gas for radiation of frequency ν is $\kappa\ \mathrm{cm^2 gm^{-1}}$, the flow of radiation through the gas is governed by the equation of radiation transfer

$$\frac{1}{\rho}\frac{dI_\nu(\vec{\Omega})}{ds} = j_\nu(\vec{\Omega}) - \kappa_\nu I_\nu(\vec{\Omega}) \tag{2.1}$$

where s denotes length measured in the direction $\vec{\Omega}$.

If the gas is in local thermodynamic equilibrium, i.e., if at each point in the gas a temperature T can be defined such that the characteristics of the gas in the neighborhood of the point are those of a gas in equilibrium at that temperature, the emission coefficient j_ν is the sum of a spontaneous and induced emission term:

$$j_\nu = \kappa'_\nu B_\nu(T) + e^{-\frac{h\nu}{kT}} \kappa_\nu I_\nu \tag{2.2}$$

where

$$\kappa'_\nu = \kappa_\nu \left(1 - e^{-\frac{h\nu}{kT}}\right) \tag{2.3}$$

and B_ν is the Planck distribution function, which is the value I_ν would have within an enclosure in thermodynamic equilibrium at temperature T. The following discussion is limited to gases in local thermodynamic equilibrium.

Substitution of Eq. (2.2) into Eq. (2.1) yields

$$\frac{1}{\rho}\frac{dI_\nu}{ds} = \kappa'_\nu\left(B_\nu - I_\nu\right) \tag{2.4}$$

From this equation it is clear that one parameter characteristic of the gas suffices to specify completely its radiative properties, namely

$$\mu'_\nu = \rho\kappa'_\nu \tag{2.5}$$

the absorption coefficient of the gas.

In many problems the spectral distribution of the radiation is not of primary concern. For these cases an appropriately defined mean value of the absorption coefficient is useful. The manner in which the mean value is calculated depends on the characteristics of the problem under consideration. A limiting case of interest is that of an optically thin sample of gas, i.e., a sample whose dimensions are small compared with the mean free path of radiation in the gas. Consideration of this case leads to the definition of the Planck mean absorption coefficient. At the opposite extreme is the case of an optically thick gas sample, which is conveniently analyzed in terms of the Rosseland mean. These two limiting cases are discussed below, and the respective mean absorption coefficients are derived.

2.2 THE PLANCK AND ROSSELAND MEAN ABSORPTION COEFFICIENTS

Consider the radiation from an isolated thin slab of gas. The total monochromatic radiation flux per unit area leaving one face of the slab is

$$F_{\nu+} = \int_{2\pi} I_\nu \cos\Theta \, d\Omega \tag{2.6}$$

where Θ is measured from the normal to the slab. Multiplying Eq. (2.4) on both sides by $d\Omega$ and integrating over the hemisphere of outward directions yields the equation

$$\int \frac{d\bar{I}_\nu}{dx} \cos\Theta \, d\Omega = 2\pi \mu_\nu' B_\nu - \mu_\nu' \int I_\nu \, d\Omega \qquad (2.7)$$

where x is distance normal to the slab face. From Eq. (2.6) and the definition of the mean outward intensity (Ref. 4, Equation 3.43)

$$\bar{\bar{I}}_{\nu+} = \frac{1}{2\pi} \int_{2\pi} I_\nu \, d\Omega$$

Eq. (2.7) may be rewritten

$$\frac{dF_{\nu+}}{dx} = 2\pi \mu_\nu' \left(B_\nu - \bar{\bar{I}}_{\nu+} \right) \qquad (2.8)$$

Our thin slab approximation now consists in neglecting $\bar{\bar{I}}_{\nu+}$ relative to B_ν, and taking $\frac{dF_{\nu+}}{dx}$ as the ratio of finite increments of emitted flux δF and slab thickness δx. With these approximations, we obtain from Eq. (2.8) for the integrated flux or total radiant energy emitted

$$\delta F \cong 2\pi \, \delta x \int \mu_\nu' B_\nu \, d\nu \qquad (2.9)$$

The corresponding radiation emitted by a perfect radiator in equilibrium at temperature T is σT^4. The emissivity ϵ of the gas is the ratio of its total radiation to that emitted by a black body at the same temperature; hence

$$\epsilon = \frac{2\pi \, \delta x \int \mu_\nu' B_\nu \, d\nu}{\sigma T^4} \qquad (2.10)$$

The quantity $\frac{\epsilon}{\delta x}$, the emissivity per unit length, is usually quoted. It can be written as

$$\frac{\epsilon}{\delta x} = \frac{2\pi}{\sigma T^4} \int \mu_\nu' B_\nu(T)\, d\nu = 2\, \bar{\mu}_e(T) \tag{2.11}$$

where

$$\bar{\mu}_e(T) = \frac{\int \mu_\nu' B_\nu(T)\, d\nu}{\int B_\nu(T)\, d\nu} = \frac{\pi \int \mu_\nu' B_\nu(T)\, d\nu}{\sigma T^4} \tag{2.12}$$

is the Planck mean absorption coefficient, sometimes referred to as the emission mean absorption coefficient.

Now consider the case where the dimensions of the gas sample are large compared with the mean free path, so that radiation cannot move freely from one part of the gas to another. To first approximation we take

$$I_\nu \cong B_\nu \tag{2.13}$$

Substituting for I_ν in the transport equation, in the derivative only, gives

$$I_\nu = B_\nu - \frac{dI_\nu}{\mu_\nu' ds} \cong B_\nu - \frac{dB_\nu}{\mu_\nu' ds} \tag{2.14}$$

and re-substitution would produce higher order terms. Since B_ν is isotropic, the expression for the x component of the flux reduces to:

$$F_x = \int_\nu \int_\Omega I_\nu \cos\Theta\, d\Omega\, d\nu = \int_\nu \int_\Omega \frac{1}{\mu_\nu'} \cdot \frac{dB_\nu}{dT} \frac{dT}{dx} \cos^2\Theta \sin\Theta\, d\Theta\, d\phi\, d\nu$$

$$\therefore = -\frac{4\pi}{3} \frac{1}{\bar{\mu}_R} \frac{dT}{dx} \int_\nu \frac{dB_\nu}{dT} d\nu = -\frac{4\pi}{3} \frac{1}{\bar{\mu}_R} \frac{dB(T)}{dx} \tag{2.15}$$

where Θ is measured from the x axis, $B(T)$ is the integrated Planck intensity, and

$$\frac{1}{\bar{\mu}_R} = \frac{\int \frac{1}{\mu'_\nu} \frac{dB_\nu}{dT} d\nu}{\int \frac{dB_\nu}{dT} d\nu} \tag{2.16}$$

defines $\bar{\mu}_R$, the Rosseland mean absorption coefficient. Related quantities are the Rosseland mean opacity, defined as $\bar{\kappa}_R = \frac{\bar{\mu}_R}{\rho}$, and the Rosseland mean free path $\Lambda_R = \frac{1}{\bar{\mu}_R}$.

Equation (2.15) may then be written in the form

$$\vec{F} = -\frac{4\pi}{3} \Lambda_R \vec{\nabla} B(T) \tag{2.17}$$

The condition for validity of Eq. (2.15) and (2.17) is that the fractional variation in temperature be small in a distance of one mean free path for all frequencies of interest; hence

$$\frac{1}{\mu'_\nu} \frac{|\vec{\nabla} T|}{T} << 1 \tag{2.18}$$

2.3 IMPORTANCE OF LINE WIDTHS IN RADIATION TRANSPORT

The importance of line effects in radiation transport can be illustrated most easily in the two opposite limits of the optical depth for which simple solutions to the transport equation exist, namely, in the limit of an optically thin sample and in the limit of an optically thick sample. These two cases were discussed in Section 2.2. Consider first the optically dense case where the Rosseland mean absorption coefficient [Eq. (2.16)] becomes a useful parameter. The Rosseland mean is an inverse mean and thus depends critically on the minimum values of $\mu(\nu)$, the so-called "windows." Conversely, it is relatively insensitive to the intensities at the peaks of the lines,

especially for strong lines. The most important characteristic of the strong line is, in the optically thick case, the width over which it effectively blacks out the spectrum.

In the case of an optically thin sample the useful parameter is the Planck mean absorption coefficient [Eq. (2.12)]. Assuming the lines to be sufficiently narrow so that the factor

$$\nu^3 e^{-\frac{h\nu}{kT}}$$

does not change appreciably across the width of a line, we see that the line shape is clearly unimportant. Each line can be considered a delta function and the frequency integration performed immediately. It follows that the Planck mean is an additive mean and, as such, can be used to estimate the gross, overall contribution of the lines to the total absorption coefficient.

The evaluation for the intermediate case cannot be simply determined, but one must resort to a detailed transport calculation to determine the sensitivity to the widths and shapes of the lines. A calculation has been carried out to estimate the effect of line widths on a transport problem. This calculation will be described in Section 5.

Section 3
THE LINE ABSORPTION COEFFICIENT OF AIR

3.1 EXPRESSION FOR THE ABSORPTION COEFFICIENT OF A SINGLE LINE

We first derive an expression for the absorption coefficient for a single "pure" line, that is, a line arising from a transition between non-degenerate electronic levels or sub-levels.* In the following it will be assumed that the reader has a reasonable familiarity with conventional spectroscopic notation and with the theory of the spectra of diatomic molecules on a level, say, with that in Herzberg's text, Spectra of Diatomic Molecules (Ref. 5). For the reader's convenience, however, we have included some background material in Section 4.

The line absorption coefficient $\mu(\nu)$ for a transition from a lower state (n'', v'', J'') to an upper state (n', v', J') is given by**

$$\mu(\nu) = N_{n''v''J''} B_{n''n',v''v',J''J'} h\nu_{n''n',v''v',J''J'} F(\nu) \qquad (3.1)$$

where

$\nu_{n''n',v''v',J''J'}$ = Bohr frequency (measured in cm^{-1}) of the line

$N_{n''v''J''}$ = particle density in the lower state (n'', v'', J'')

$B_{n''n',v''v',J''J'}$ = Einstein coefficient for induced absorption

$F(\nu)$ = a line shape factor such that $\int F(\nu)\, d\nu = 1$.

*By sub-level we simply mean one of the components of a degenerate electronic state, for example, one of the $2S+1$ components of a Σ state with spin S or one of the components of a Λ-type doublet. By electronic degeneracy we mean the spin and orbital degeneracy that would exist in the absence of nuclear motion (rotation and vibration), spin-orbit interactions, and electron spin interactions. (We ignore completely any interaction of the nuclear spins with the rest of the molecule.) The $2J+1$ spatial degeneracy associated with molecular rotation, which rigorously exists in an isotropic environment, is never counted in figuring electronic degeneracy.

**Double and single primes will be used to denote lower and upper states, respectively.

Here n is used to denote a non-degenerate electronic level or sub-level, while v and J denote vibrational and rotational levels, respectively.

The Einstein coefficient $B_{n''n',v''v',J''J'}$ is given by

$$B_{n''n',v''v',J''J'} = \frac{8\pi^3}{3h^2c} \frac{\sum_{M''M'} \left| R^{M''M'} \right|^2}{2J'' + 1} \tag{3.2}$$

where

$$R^{M''M'} = \int \Psi''_{n''v''J''M''} \vec{R} \Psi'_{n'v'J'M'} \, d\tau \tag{3.3}$$

is the matrix element of the electric moment operator $\vec{R} = \vec{R}_e + \vec{R}_n$ of the electrons and nuclei. M'' and M' are azimuthal quantum numbers numbering the (spatially) degenerate rotational levels of the lower and upper states, respectively. The summation in Eq. (3.2) is over all possible combinations of the rotational sub-levels of the lower with those of the upper state. If we assume the Born-Oppenheimer approximation to be valid, the molecular wave function may be separated into electronic, vibrational, and rotational parts

$$\Psi = \Psi_e \Psi_v \Psi_r \tag{3.4}$$

The vibrational eigenfunction Ψ_v depends on the internuclear distance only. The electronic eigenfunction Ψ_e depends on the electron coordinate and slightly on the internuclear distance as a parameter. The rotational eigenfunction Ψ_r depends on the nuclear coordinates and, in the general case, also on the electron coordinates, inasmuch as the quantum number J' here refers to the total angular momentum resulting from nuclear rotation and, if present, electron spin and orbital angular momentum.

By substituting Eq. (3.4) into Eq. (3.3), it is readily shown that

$$\left| R^{M'' M'} \right|^2 = \left| \bar{R}_e \right|^2 q(v'v'') \, S_{\bar{J}} \tag{3.5}$$

where

$$\left| \bar{R}_e \right|^2 = \left| \int \Psi_e' \, \vec{R}_e \, \Psi_e'' \, dt_e \right|^2 \tag{3.6}$$

$$q(v'v'') = \left| \int \Psi_v' \, \Psi_v'' \, dt_v \right|^2 \tag{3.7}$$

Here, $S_{\bar{J}''}$ is a line strength factor and is that part of $\Sigma \left| R^{\bar{M}' \bar{M}''} \right|^2$ that depends on $\bar{J}''$ (and also on Λ, the component of the electronic orbital angular momentum along the internuclear axis, whenever $\Lambda \neq 0$). $S_{\bar{J}}$ is usually called the Hönl-London intensity factor. Hönl-London factors for all the important types of electronic transitions are available in the literature. R_e is the electronic transition moment which, in general, depends on the internuclear separation. $q(v'v'')$ is the so-called Franck-Condon factor for the (v', v'') band.

Equation (3.2) then becomes

$$B_{n''n', v''v', J''J'} = \frac{8\pi^3}{3h^2 c} \left| R_e \right|^2 q(v'v'') \, \frac{S_{J''}}{2J''+1} \tag{3.8}$$

The particle density $N_{n''v''J''}$ in a level (n'', v'', J'') is given by

$$N_{n''v''J''} = N_{total} \, \frac{(2J''+1)\, \omega_I \exp\left(-E_{n''v''J''}/kT\right)}{Q_{total}} \tag{3.9}$$

where N_{total} is the total particle density for all levels, $E_{n''v''J''}$ is the energy of the level, ω_I is the nuclear spin statistical weight for this level, and Q_{total} is the total partition function for the system.

The total partition function may be written as a sum of contributions from each electronic state:

$$Q_{total} = \sum_{n} Q_n \tag{3.10}$$

where n denotes the electronic state. Taking into account electronic (orbital + spin), vibrational, rotational, and nuclear (spin only) degrees of freedom, we may write Q_n in the form

$$Q_n = Q_{electronic}\, Q_{vib-rot.}\, Q_{nuclear} \tag{3.11}$$

where

$$Q_{electronic} = \omega_\Lambda (2S + 1) \exp\left(\frac{-\nu_{oo} hc}{kT}\right); \quad \omega_\Lambda = 1 \text{ if } \Lambda = 0, \quad \omega_\Lambda = 2 \text{ if } \Lambda \neq 0 \tag{3.12}$$

$$Q_{vib-rot.} = \sum_{v=o}^{\infty} \exp\left[\frac{-G_o(v)\, hc}{kT}\right] Q_{rot.}^{(v)} \tag{3.13}$$

$$Q_{rot.}^{(v)} = \int_{o}^{\infty} (2J+1) \exp\left[\frac{-F_v(J)\, hc}{kT}\right] dJ \approx \frac{kT}{hcB} \tag{3.14}$$

$$Q_{nuclear} = \frac{(2I_a + 1)(2I_b + 1)}{\sigma} \tag{3.15}$$

In these formulas, ν_{oo} is the energy of the lowest vibrational level of electronic state n above that of the ground state, $G_o(v)$ is the vibrational term referred to the lowest vibrational level as zero, $F_v(J)$ is the rotational term for the v^{th} vibrational level and B_v is the corresponding rotational constant, ω_Λ is the statistical weight for orbital angular momentum (Λ) about the internuclear axis, S is the total spin of

the electrons, I_a and I_b are the nuclear spins of the two nuclei a and b, respectively, and σ is a symmetry number having the value 2 for homonuclear molecules and 1 for heteronuclear systems.

An approximate formula for $Q_{vib-rot.}$ that is somewhat easier to use than Eqs. (3.13) and (3.14) and yet entirely adequate for our purposes has been given by Bethe (Ref. 6) and later corrected by Brinkerly (Ref. 7):

$$Q_{vib-rot.} = \frac{1}{1 - \exp(-1.4388\ \omega_o/T)}\ \frac{T}{1.4388\ B_o}\ (1+\gamma T) \tag{3.16}$$

where γ, Bethe's correction factor for anharmonicity and non-rigidity, has the value

$$\gamma = \frac{1}{1.4388\ \omega_o}\left(\frac{2\,\omega_o X_o}{\omega_o} + \frac{\alpha_o}{B_o} + \frac{8B_o}{\omega_o}\right) \tag{3.17}$$

Here ω_o and B_o are the vibrational and rotational constants of the $v = o$ vibrational level, $\omega_o X_o$ is the first anharmonic constant and α_o is the interaction constant for coupling between rotation and vibration (Ref. 5).

Returning now to Eq. (3.9) we multiply numerator and denominator by Q_n as given by Eqs. (3.11 – 3.15) and obtain after some manipulation

$$N_{n''v''J''} = \left[N_{total}\ \frac{Q_{n''}}{Q_{total}}\right]\ \frac{1}{\omega_\Lambda\ (2S+1)}\ \frac{\omega_I}{Q_{nuclear}}\ \times \tag{3.18}$$

$$\frac{(2J''+1)\ \exp\left[-\left\{G_o(v'') + F_{v''}(J'')\right\} hc/kT\right]}{Q_{vib-rot.}}$$

where use has been made of the relation

$$E_{n''v''J''} = \left[\nu_{oo} + G_o(v'') + F_{v''}(J'')\right] hc \tag{3.19}$$

Substituting Eq. (3.8) for $B_{n''n',v''v',J''J'}$ and Eq. (3.18) for $N_{n''v''J''}$ into Eq. (3.1) we obtain the following rather complicated expression for the line absorption coefficient:

$$\mu(\nu) = \left[N_{total}\, P_{n''}\right] \frac{8\pi^3\, \omega_I}{3hc\, Q_{nuclear}\, \omega_\Lambda (2S+1)}\, \nu_{n'',n',v'',v',J'',J'} \left|R_e\right|^2 q(v',v'')\, S_{J''} \frac{\exp\left[-\left\{G_o''(v'') + F_{v''}''(J'')\right\}\frac{hc}{kT}\right]}{Q_{vib-rot.}} F(\nu) \tag{3.20}$$

where $P_{n''} = Q_{n''}/Q_{total}$ is the fractional population of the n''^{th} electronic state. By introduction of the notation

$$H_{n''n',v''v',J''J'} = \frac{8\pi^2\, L_o}{3hc} \frac{\omega_I}{\omega_\Lambda (2S+1)\, Q_{nuclear}}\, \nu_{n''n',v''v',J''J'} \left|R_e\right|^2 q(v'v'')\, S_{J''} \tag{3.21}$$

$$E_{v''J''} = \left[G_o''(v'') + F_{v''}''(J'')\right] hc/k \tag{3.22}$$

where $L_o = 2.6875 \times 10^{19}$ particles/cm^3 is Loschmidt's Number, Eq. (3.22) becomes

$$\mu(\nu) = \left[\frac{N_{total}\, P_{n''}}{L_o\, Q_{vib-rot.}}\right] H_{n''n',v''v',J''J'} \exp\left(-E_{v''J''}/T\right) \pi F(\nu) \tag{3.23}$$

Note that the quantities H and E are characteristic of the isolated molecule, that is, do not depend on the temperature and density. Note that the bracketed term in Eq. (3.23) is dimensionless and that H has the dimensions cm^{-2}. Since the shape factor $F(\nu)$ has dimensions cm (see below), $\mu(\nu)$ has the dimension cm^{-1} as required.

Although Eq. (3.23) remains valid for arbitrary form factor $F(\nu)$, in all of our work we have assumed a Lorentz line profile, viz.,

$$F(\nu) = \frac{1}{\pi} \frac{\sigma}{\sigma^2 + \left(\nu - \nu_{n''n', v''v', J''J'}\right)^2} \tag{3.24}$$

where σ is the line half-width at half-maximum.

3.2 OVERLAPPING AND COMPOSITE LINES

The absorption coefficient $\mu(\nu)$ at ν due to several overlapping lines is, of course, the sum of the separate line absorption coefficients:

$$\mu(\nu) = \sum_i \mu_i(\nu) \tag{3.25}$$

where i labels the lines and the sum runs over all the lines whose profiles overlap significantly at ν.

Fine structure may frequently be ignored without compromising the accuracy of the calculation. In these cases the intensity factor of the unresolved line may be obtained by combining the intensity factors of the unresolved components. An example of the construction of such an intensity factor will be included in Section 4.5.

Section 4

THE LINE FREQUENCIES AND LINE INTENSITIES FOR AIR

4.1 SPECTROSCOPIC QUANTUM NUMBERS

In a diatomic molecule, the symmetry of the field in which the electrons move is axial about the line connecting the two nuclei, with the component of the orbital angular momentum of the electrons about the internuclear axis being a constant of the motion. The orbital angular momentum, $\bar{L}$, precesses about this axis with constant component $M_L \hbar$, where M_L is restricted to the values $M_L = L, L-1, L-2, \cdots, -L$. Since, in diatomic molecules, states differing only in the sign of M_L have the same energy (are degenerate), it is appropriate to introduce the quantum number

$$\Lambda = |M_L| \; ; \; = 0, 1, 2, \cdots -L .$$

If $\bar{L}$ precesses very rapidly, its meaning as angular momentum may be lost, but M_L and Λ remain well defined.

When $\Lambda = 0, 1, 2, 3, \cdots$, the corresponding molecular state is designated a Σ, Π, Δ, Φ, $\cdots$ state, analogous to the mode of designation for atoms. By convention, Greek letters refer to the components of electronic angular momenta, while the corresponding lower case letters used for atoms refer to the electronic angular momenta themselves. Π, Δ, Φ, $\cdots$ states are doubly degenerate since M_L can have the two values $+\Lambda$ and $-\Lambda$. Σ states are non-degenerate.

Just as for atoms, the spins of the electrons form a resultant $\bar{S}$, the corresponding quantum number S being integral or half integral as determined by whether the total number of electrons in the molecule is even or odd. The component of $\bar{S}$ along the axis of symmetry is designated Σ (analogous to atoms), and this must not be confused with the Σ which means $\Lambda = 0$. The values allowed Σ are $S, S-1, S-2, \cdots -S$,

i.e., $2S + 1$ different values are possible. The quantum number Σ can be either positive or negative, except it is not defined when $\Lambda = 0$ (for Σ-states).

The total electronic angular momentum about the internuclear axis is obtained by an algebraic addition of Λ and Σ. The resultant quantum number is given by $\Omega = |\Lambda + \Sigma|$. If $\Lambda \neq 0$, there are $2S + 1$ values of $\Lambda + \Sigma$ for a given value of Λ. The interaction of S with the magnetic field produced by Λ gives rise to a multiplet structure. The term symbol carries $2S + 1$ as a left superscript and $\Lambda + \Sigma$ as a right subscript, for example the triplet ${}^3\Delta$ would have components ${}^3\Delta_3$, ${}^3\Delta_2$, and ${}^3\Delta_1$. Even for Σ states (there is no magnetic field in the direction of the internuclear axis) the multiplicity is said to be $2S + 1$ even though no actual splitting may occur for non-rotating molecules.

4.2 SYMMETRY PROPERTIES OF THE EIGENFUNCTIONS

Under the coordinate transformation $x_k \longrightarrow -x_k$, $y_k \longrightarrow -y_k$, $z_k \longrightarrow -z_k$, the wave function for any atomic system either changes sign or remains unchanged in sign. For a rigid rotator, a reflection at the origin is accomplished by the transformation $\Theta \longrightarrow \pi - \Theta$, $\Phi \longrightarrow \pi + \Phi$. It turns out that the rotator wave function remains unchanged for even J and changes sign for odd J. In the case of the symmetric top ($\Lambda \neq 0$), each rotational level is doubly degenerate. Linear combinations that change sign or remain unchanged under reflection can always be chosen, however.

The rotational levels of a diatomic molecule are classified according to their behavior under reflection of the total wave function (not just the rotational wave function alone). A rotational level is called positive or negative depending on whether the total wave function remains unchanged or changes sign for reflection at the origin. To a first approximation, the total wave function for a diatomic molecule can be written

$$\Psi = \Psi_e \Psi_v \Psi_r \qquad (4.1)$$

Since it depends only on the magnitude of the internuclear distance, Ψ_v remains unchanged under reflection. Consider now two cases, $\Lambda = 0$ and $\Lambda \neq 0$.

4.2.1 Case: $\Lambda = 0$

If Ψ_e remains unchanged under reflection, the parity depends only on Ψ_r and the rotational levels are + or - , depending on whether J is even or odd. (See below.) If Ψ_e changes sign under reflection, however, the total wave function remains unchanged for odd J and changes sign for even J . In this case odd J levels are positive and even J levels are negative:

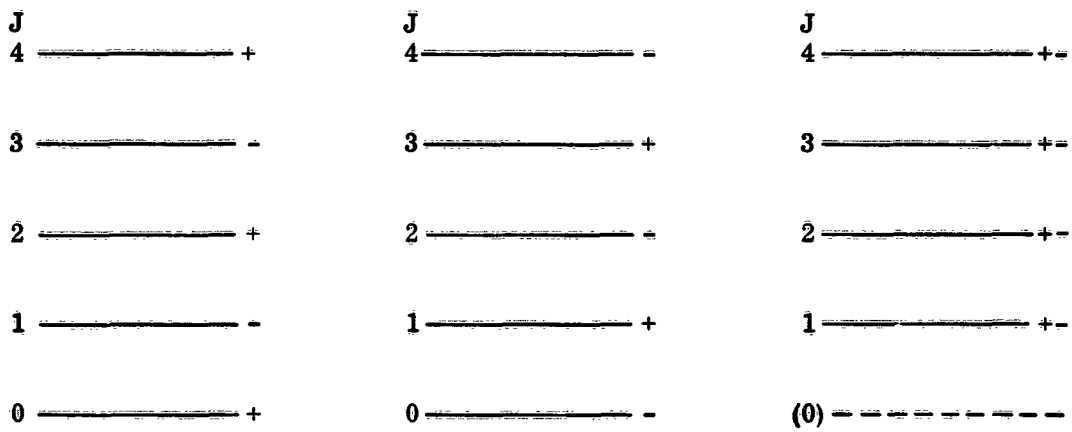

Case: $\Lambda = 0$ $\quad \Psi_e = I\Psi_e$

Case: $\Lambda = 0$ $\quad \Psi_e = -I\Psi_e$

Case: $\Lambda = 1$ $\quad \Psi_e = \pm I\Psi_e$

Energy Level Diagram

(I is the operator which replaces $\vec{r}$ by $-\vec{r}$)

4.2.2 Case: $\Lambda \neq 0$

In this case for each value of J there are positive and negative rotational levels of equal energy. (See above.) The levels are drawn as if they were degenerate. Actually, when account is taken of the interaction between electronic motion and rotation, there is a slight splitting of the degeneracy. Note that the $J = 0$ level cannot occur for $\Lambda = 1$, since J here is the total (rotational plus orbital) angular momentum.

It must be emphasized that the positive or negative character of the rotational levels depends only on the rotational symmetry of the system, i.e., equivalence of right and

left-handed coordinate systems, and has nothing to do with the approximate representation of the total wave function given by Eq. (4.1). This approximation was introduced only for the purpose of determining which levels are positive and which are negative. It will be shown below that positive levels combine only with negative levels under dipole radiation and vice versa. Symbolically

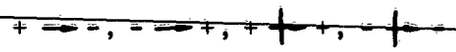

Clearly, this is compatible with the selection rule $\Delta J = \pm 1$ for the simple rotator or $\Delta J = 0, \pm 1$ for the symmetric top rotator with $\Lambda \neq 0$.

The opposite selection rule holds for the Raman effect: + terms combine only with + and - only with -, or symbolically

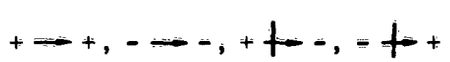

which is consistent with the selection rule $\Delta J = 0, \pm 2$ for the simple rotator or $\Delta J = 0, \pm 1, \pm 2$ for a symmetric top with $\Lambda \neq 0$.

Selection rules for dipole radiation depend on integrals of the form

$$\int \Psi_n^* \vec{M} \Psi_m \, d\tau$$

Now $\vec{M} = -I\vec{M}$. If both Ψ_n and Ψ_m are positive or both negative under reflection, the integral will change sign. This is only possible if the integral is identically zero, i.e., such transitions are forbidden. On the other hand, transitions between positive and negative levels are allowed since the sign of the integral does not change under reflection.

The Raman rule follows in the same way by noting that the polarizability is unchanged under reflection.

For homonuclear molecules rotational levels may be further classified according to their behavior under interchange of the two identical nuclei. In the same way as one shows that, for the exchange of two electrons, the total wave function must either change sign or remain unchanged in sign, we can show that for an exchange of nuclei the total wave function either remains unchanged in sign or changes only its sign, in which case the state under consideration is said to be symmetric or antisymmetric in the nuclei, respectively. We can also show that in a given electronic state either the positive rotational levels are symmetric and the negative are antisymmetric throughout, or the positive rotational levels are antisymmetric and the negative are symmetric throughout. As an example consider the case $\Lambda = 0$. Clearly there are four cases:

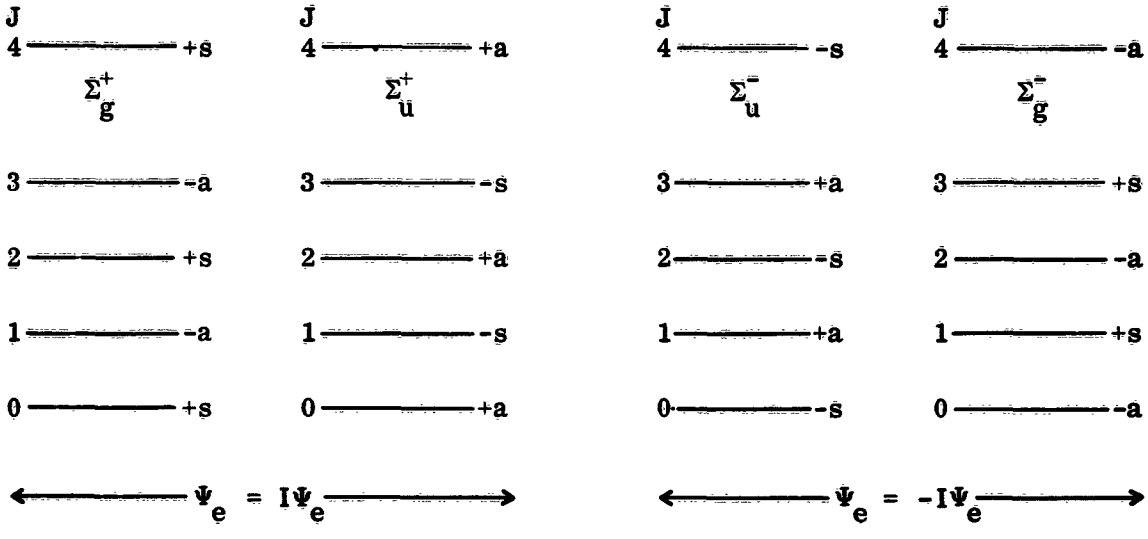

$\Lambda = 0$

If the nuclei have zero nuclear spin (or if the interaction between nuclear spin with the rest of the molecule is neglected), there is a rigorous prohibition of intercombination between symmetric and antisymmetric states:

This holds for transitions brought about in any way, e.g., collisions, Raman effect, dipole radiation, etc. The proof of this follows trivially from the form of the operator for the type of transition involved. Physically, operators for dipole radiation, collisions, Raman effect, etc., must be symmetric in the two nuclei. Since transition probabilities are governed by integrals of the form

$$\int \Psi_m^* \, O \, \Psi_m \, d\tau$$

it follows the Ψ_n and Ψ_m must transform in the same way for interchange of the nuclei.

An immediate consequence of the non-intercombination rule is that there are no vibration-rotation or rotational spectra for homonuclear diatomic molecules since two rotational levels for which the selection rule $\Delta J = \pm 1$ is fulfilled have opposite symmetry in the nuclei. Raman effect transitions can occur, however, with $\Delta J = 0, \pm 2$.

For quadrupole radiation, $\Delta J = 0, \pm 1, \pm 2$. It is seen that $\Delta J = 0, \pm 2$ is compatible with a—|—s and therefore this type of radiation can occur in homonuclear molecules.

4.3 COUPLING OF THE ANGULAR MOMENTA

There are mutual interactions between the electronic, vibrational, and rotational motions of a diatomic molecule. The electronic-vibrational interaction is taken into account by choosing the vibrational levels to fit the electronic potential curve; the vibrational-rotational interaction is accounted for by considering the molecule to be a vibrating rotator. Mutual interaction of the electronic and rotational motions must be considered also; this interaction depends on which quantum numbers distinguish the rotational levels in different types of electronic states, and on the energy dependence on the quantum numbers.

Angular momenta in the molecule combine to form a resultant designated $\bar{J}$. The spin $\bar{S}$, nuclear rotation $\bar{N}$, and orbital angular mementum Λ are coupled in different ways to form $\bar{J}$. The modes of coupling were classified by Hund and are called Hund's case "a," "b," "c," --- etc. Of these we need discuss only two, cases "a" and "b."

4.3.1 Hund's Case "a"

In Hund's case "a" it is assumed that the interaction of the nuclear rotation with the electronic motion (orbital + spin) is very weak, whereas the electronic motion is strongly coupled to the internuclear axis (see Fig. 4-1).

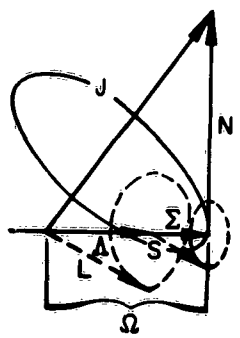

Fig. 4-1
Hund's Case "a"

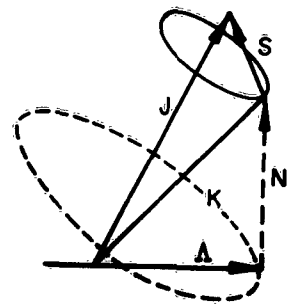

Fig. 4-2
Hund's Case "b"

The total electronic angular momentum Ω is then well defined. Ω and N combine to form J. The precession of L and S about the internuclear axis is assumed to be very much faster than the nutation of the figure axis. Ω is integral or half-integral, depending on whether the number of electrons is even or odd. Since J cannot be smaller than its component Ω,

$$J = \Omega, \ \Omega + 1, \ \Omega + 2, \cdots$$

Levels with $J < \Omega$ do not occur.

4.3.2 Hund's Case "b"

When the spin is not coupled to the internuclear axis at all, Ω is not defined and Hund's case "a" cannot apply. This is true where $\Lambda = 0$ and $S \neq 0$ and may be nearly true in other instances. In Hund's case "b," therefore, the spin is decoupled from the internuclear axis or is very weakly coupled to it. Λ and N form a resultant K, which then combines with S to form a resultant J (Fig. 4-2). If $\Lambda = 0$, K is identical with N and is therefore perpendicular to the internuclear axis. In general K may have the integral values $K = \Lambda, \Lambda + 1, \Lambda + 2, \cdots\cdots$. The possible values of J are $(K+S), (K+S-1), (K+S-2), \cdots |K-S|$; for a given K. Except when $K < S$, then, each level of a given K consists of $2S+1$ components. Again J is half-integral or integral according to whether the number of electrons is odd or even, respectively.

Λ Type Doubling

In Hund's cases "a" and "b," the interaction between N and L has been neglected. For larger speeds of rotation this interaction must be taken into account and is found to produce a splitting into two components for each J value in states with $\Lambda \neq 0$ which are doubly degenerate when there is no rotation. This splitting, which is present in all states where $\Lambda \neq 0$ and increases with increasing rotation (J), is called Λ-type doubling.

Spin Uncoupling

It may occur (and frequently does) that a molecule coupled according to Hund's case "a" for small J may, with increasing rotation, go over to case "b." This happens when the rotational velocity of the molecule becomes large compared with the precessional velocity of S about Λ. S then is essentially decoupled so that Ω is not defined but K is. This process is called spin uncoupling. It is often convenient to formally extend the quantum number K back to small rotation values even though it is not, strictly speaking, defined.

4.4 SELECTION RULES AND BRANCHES

$\bar{J}$, the quantum number of the total angular momentum, obeys the selection rule $\Delta\bar{J} = 0, +1, -1$ with the restriction that $\Delta\bar{J} = 0$ is forbidden when $\Lambda = 0$ in both the upper and the lower electronic states. This selection rule forms a basis for classifying the spectral lines into distinct series called branches, $\bar{J}' = \bar{J}'' + 1$ corresponding to the R-branch, $\bar{J}' = \bar{J}'' - 1$ to the P-branch, and $\bar{J}' = \bar{J}''$ to the Q-branch. Thus the rotational contribution to the frequency of a transition by the branches can be expressed as

$$P(\bar{J}) = \bar{F}'(\bar{J} - 1) - \bar{F}''(\bar{J})$$

$$Q(\bar{J}) = \bar{F}'(\bar{J}) - \bar{F}''(\bar{J})$$

$$R(\bar{J}) = \bar{F}'(\bar{J} + 1) - \bar{F}''(\bar{J})$$

The above are called main branches to distinguish them from satellite branches. For illustration, assume that both the upper and the lower state take case "b" coupling. Then the relevant quantum numbers are K, S, and $\bar{J}$. The transitions with $\Delta\bar{J} = \Delta K$ are the main branches, and those with $\Delta\bar{J} \neq \Delta K$ are the satellite branches. The satellite branches always lie close to the main branches and are usually much weaker. If, for example, the transition takes place between a $^2\Pi(b)$ and a $^2\Sigma^+$ state, with $\bar{J}' = \bar{J}''$ and $K' = K'' + 1$, then this transition is called an R-form Q satellite branch and is abbreviated ^{R}Q. It is a Q branch because $\bar{J}' = \bar{J}''$ and r-form because $K' = K'' + 1$.

Various other selection rules arise from the symmetries in a dynamical system. For example, the requirement that the total wave function for a molecule can,at most,change sign for an inversion of the coordinates of all the particles leads to the rule that in the dipole approximation transitions can take place only between rotational levels of opposite sign. If the nuclei of a diatomic molecule are identical, an exchange of the nuclei should either leave the total wave function unchanged or change its sign for symmetric or antisymmetric states. The corresponding general selection rule prohibits transitions between symmetric and antisymmetric states. When the two nuclei

are not identical but do have the same charge, the electronic wave function should suffer at most a change of sign when the coordinates of the electrons are changed in sign. If the electronic wave function does not change sign, the total molecular wave function is "even" or "gerade." Otherwise it is "odd" or "ungerade." Even states do not combine with even states, nor odd with odd.

There are other selection rules which are not valid in general, but which hold to the extent that the intra-molecular interactions can be represented by one of Hund's ideal coupling cases. When each state participating in a transition belongs either to case "a" or to case "b," then Λ, the projected electronic orbital angular momentum, obeys the selection rule $\Delta\Lambda = 0, +1, -1$ as long as the spin-orbit and rotation-electronic motion interactions are small. When $\Lambda = 0$ for both states, there is the further rule that the sign of the state cannot change:

$$\Sigma^+ \not\longleftrightarrow \Sigma^+ \quad , \quad \Sigma^- \not\longleftrightarrow \Sigma^- \quad , \quad \text{but not} \quad \Sigma^+ \longleftrightarrow \Sigma^-$$

Violations of the above rule occur when the rotation-electronic motion interaction cannot be regarded as small. If the spin-orbit interaction is small, there is also a selection rule for S, namely that $\Delta S = 0$.

In the special circumstance that both the upper and the lower state belong to case "a," the following two selection rules hold:

$$\Delta\Sigma = 0$$

$$\Delta\Omega = 0, +1, -1 \quad (\text{but not } \Omega = 0 \not\rightarrow \Omega = 0)$$

The first of these rules holds only for small spin orbit interaction, but the second is not so restricted.

If both the upper and the lower states belong to case "b," then K, the quantum number for the total angular momentum apart from the spin, obeys the following rule

$$\Delta K = 0, +1, -1 \text{ (but not } K = 0 \rightarrow K = 0 \text{ for } \Sigma \rightarrow \Sigma \text{)}$$

4.5 INTENSITY FACTORS

Tables of intensity factors (the so-called Hönl-London factors, S_J) are given by Jevons (Ref. 8, pp. 133–139) for Hund's coupling cases "a" and "b" and for various types of transitions. For intensity factors arising from other coupling conditions, refer to the discussions of the individual molecular systems. Table A-2 lists intensity factors for various transitions which are considered in the calculation.

According to the rotational sum rule, the sums of the line strengths of all the transitions from or to a given rotational level are proportional to the statistical weight of that level. This rule affords a valuable check when fine structure is to be ignored. As an example, consider a $^2\Pi - {}^2\Sigma$ transitions where the molecule is coupled according to Hund's case "b." Using the intensity factors from Table 10(ii) in Jevons (Ref. 8), we combine the factors for the lines arising from level $J'' = K' - \frac{1}{2}$:

$$R_2(K = K'' + 1) + {}^{Q}R_{12}(K = K'') + Q_2(K = K'') + {}^{P}Q_{12}(K = K'') + P_2(K = K'')$$

$$= \frac{K''(K'' + 2)}{2K'' + 1} + \frac{1}{2K'' + 1} + \frac{(K'' + 1)}{2K'' + 1} + \frac{(K'' - 1)}{4K''^2 - 1} + \frac{(K'' - 1)^2}{2K'' - 1} = 2K''$$

which is equal to the degeneracy of this level, i.e., $2J'' + 1 = 2\left(K'' - \frac{1}{2}\right) + 1 = 2K''$. For the $J'' = K'' + \frac{1}{2}$ level we obtain:

$$R_1(K = K'' + 1) + {}^{R}Q_{21}(K + K'' + 1) + Q_1(K = K'') + {}^{Q}P_{21}(K = K'') + P_1(K = K'')$$

$$= \frac{(K'' + 2)^2}{2K'' + 3} + \frac{(K'' + 2)}{(2K'' + 1)(2K'' + 3)} + \frac{K''(2K'' + 3)}{2K'' + 1} + \frac{1}{2K'' + 1} + \frac{(K'' + 1)(K'' - 1)}{2K'' + 1}$$

$$= 2(K'' + 1)$$

which is equal to the degeneracy of the level, viz., $2J'' + 1 = 2\left(K'' + \frac{1}{2}\right) + 1 = 2(K'' + 1)$. Table 10(ii) in Jevons therefore satisfies the sum rule and is presumably correct. Other results may be checked in the same fashion.

4.6 THE $B\ ^3\Sigma_u^- - X\ ^3\Sigma_g^-$ (SCHUMANN-RUNGE) SYSTEM OF O_2

4.6.1 General

With small dispersion, $^3\Sigma$-$^3\Sigma$ bands consist of a single R and a single P branch. Larger dispersion shows each line to be resolved into three components of about the same intensity. There are, thus, six main branches. Six very weak satellite branches for which $\Delta J \neq \Delta K$ are also present. Alternate triplets in the P and R branches are missing, since the nuclear spin of the oxygen atom is zero. Even K rotation levels are missing in the X state, and odd K levels are missing in the B state. In our calculation, lines will be treated as unresolved. Figure 4-3 shows two groups of lines: (R_1, R_2, R_3, $^RQ_{21}$, $^RQ_{32}$) and (P_1, P_2, P_3, $^PQ_{23}$, $^PQ_{12}$). These are considered to be composite lines whose Hönl-London factors are obtained by simply adding up the S_J's for the individual components (Ref. 8, pp. 180–181). These factors turn out to be $3K''$ for the P branch lines and $3(K'' + 1)$ for the R branch lines.

4.6.2 Line Frequencies

Rotational terms of both $^3\Sigma$ states are given by

$$F_v(K) = B_v K(K + 1) - D_v K^2(K + 1)^2$$

Table A-9 lists B_v and D_v as well as $G_o(v)$ used in the calculation. The included bands and their corresponding Franck-Condon factors are given in Table A-10.

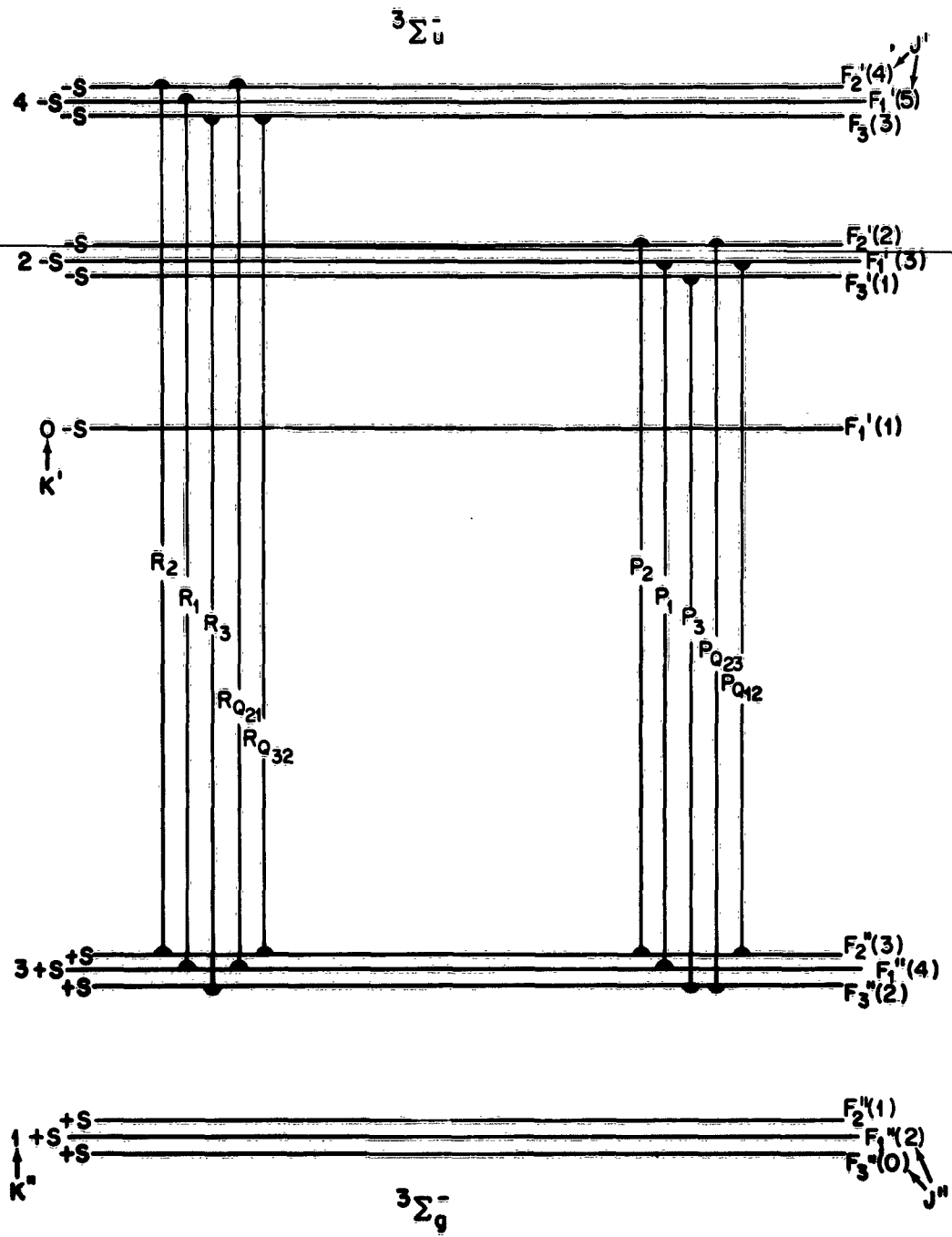

Fig. 4-3 $B\ ^3\Sigma_u^- - X\ ^3\Sigma_g^-$ Band of O_2 (Schumann-Runge System)

4.6.3 Line Intensities

For the O_2 Schumann-Runge system, then, the $H_{J'', J'}$'s are given by

$$H_{J'', J'} = H_{K'', K'} = \frac{8\pi^2 L_o}{3hc} \cdot \frac{1}{3} \left(\frac{\omega_I}{Q_{nuclear}} \right) \nu_{K'', K'} |R_e|^2 \, 2(v', v'') \, S_J$$

$$= \frac{16 \pi^2 L_o}{3hc} \nu_{K'', K'} |R_e|^2 \, q(v', v'') \cdot \begin{cases} K'' + 1 & \text{if } K' = K'' + 1 \\ K'' & \text{if } K' = K'' - 1 \end{cases}$$

where $K'' = 1, 3, 5, \ldots$

and $S_J = 3 S_K$.

4.7 THE $B^3\Pi_g - A^3\Sigma_u^+$ (FIRST POSITIVE) SYSTEM OF N_2

The structure of $^3\Pi$-$^3\Sigma$ bands is very complicated, particularly if, as is the case here, the coupling in the π state is near Hund's case "a." Since there are three sub-bands, $^3\Pi_o - {}^3\Sigma^+$, $^3\Pi_1 - {}^3\Sigma^+$, $^3\Pi_2 - {}^3\Sigma^+$, and each sub-band has nine branches (three for each triplet component of the lower state), there are, in all, 27 branches. Of these we expect 9 branches to be relatively strong (P_1, Q_1, R_1, P_2, Q_2, R_2, P_3, Q_3, R_3), ten satellite branches to be somewhat weaker, and eight to be weak branches ($^oP_{12}$, $^oQ_{13}$, $^oP_{23}$, $^sR_{21}$, $^sP_{32}$, $^sQ_{31}$, $^nP_{13}$, $^TR_{31}$). We will omit the latter eight branches entirely. The 19 remaining branches, along with their corresponding intensity factors, are listed in Table A-2. (See also Fig. 4-4.)

Formulas for the rotational levels of a $^3\Sigma$ state have been derived by Schlapp (Ref. 9):

$$F_{v1}(K) = B_v K(K+1) + (2K+3) B_v - \lambda - \sqrt{(2K+3)^2 B_v^2 + \lambda^2 - 2\lambda B_v} + \gamma(K+1)$$

$$F_{v2}(K) = B_v K(K+1)$$

$$F_{v3}(K) = B_v K(K+1) - (2K-1) B_v - \lambda + \sqrt{(2K-1)^2 B_v^2 + \lambda^2 - 2\lambda B_v} - \gamma k$$

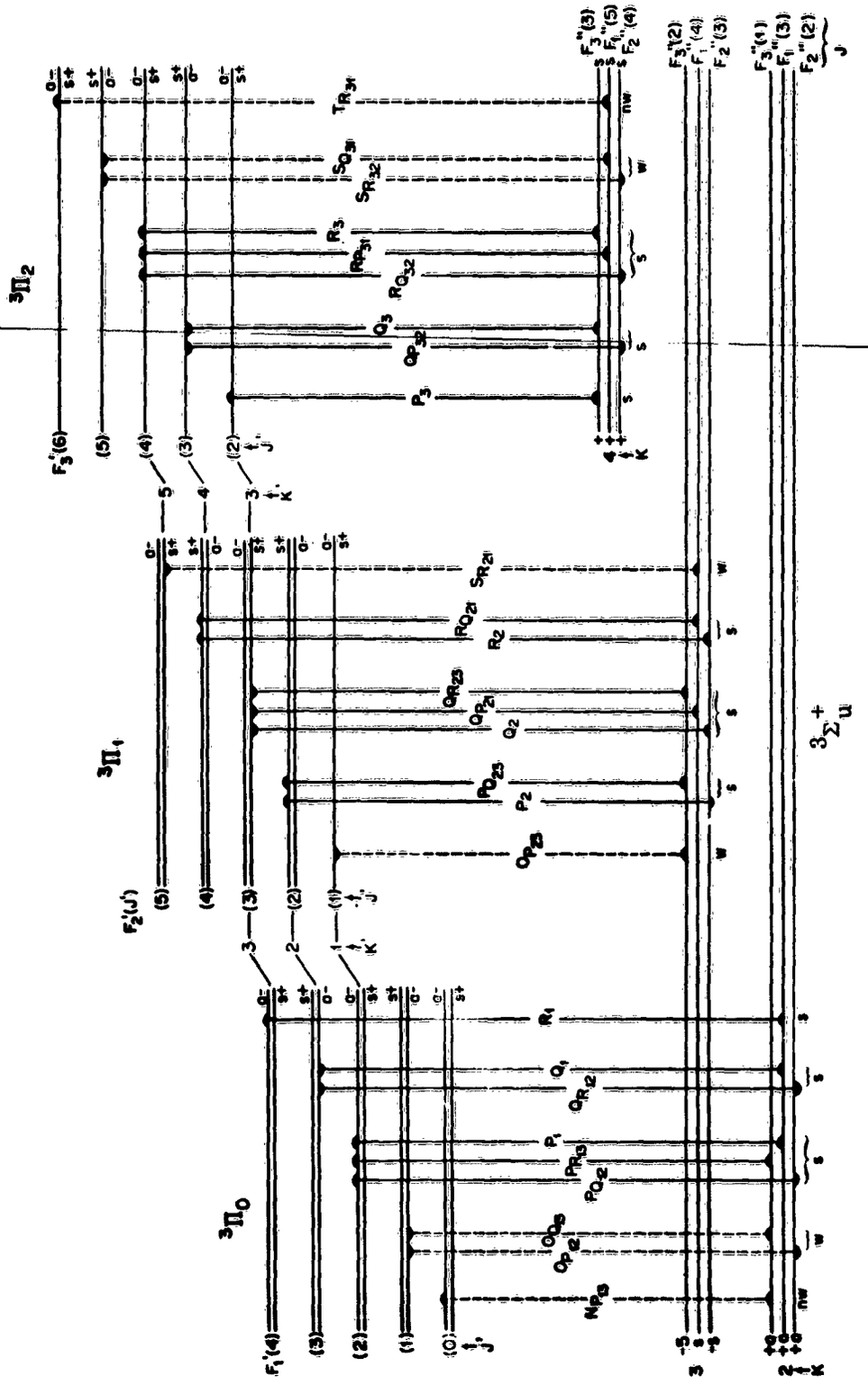

Fig. 4-4 B $^3\Pi_g$ - A $^3\Sigma_u^+$ Band of N_2 (1st Positive System)

where F_{v1}, F_{v2}, and F_{v3} refer to the levels with $J = K + 1$, K, and $K - 1$ respectively, and where λ and γ are (small) constants. From the above formulas must be subtracted the usual term $D_v K^2 (K + 1)^2$ to allow for centrifugal distortion.

Now in the case of $A^3\Sigma_u^+$ State of N_2, both splitting constants are very small and, furthermore, are known only very approximately for most of the vibrational levels. Therefore, we are justified in ignoring the spin splitting and using, instead, the term formula for $^1\Sigma$ states:

$$F_v(K) = B_v K(K + 1) - D_v K^2 (K + 1)^2$$

The values of B_v and D_v for each of the vibrational levels considered are given in Table A-3.

Rotational term formulas for the $^3\Pi_g$ state are from Budo (Refs. 10, 11) and are for any degree of uncoupling:

$$F_{v1}(J) = B_v \left[J(J + 1) - \sqrt{Z_1} - 2Z_2/3Z_1 \right] - D_v \left(J - \tfrac{1}{2} \right)^4$$

$$F_{v2}(J) = B_v \left[J(J + 1) + 4Z_2/3Z_1 \right] - D_v \left(J + \tfrac{1}{2} \right)^4$$

$$F_{v3}(J) = B_v \left[J(J + 1) + \sqrt{Z_1} - 2Z_2/3Z_1 \right] - D_v (J + 3/2)^4$$

where

$$Z_1 = Y_v(Y_v - 4) + 3/4 + 4J(J + 1)$$

$$Z_2 = Y_v(Y_v - 1) - 4/9 - 2J(J + 1)$$

and $Y_v = A_v/B_v$ is a measure of the degree of coupling of the spin to the internuclear axis. For large rotation F_{v1}, F_{v2}, and F_{v3} go over into a case "b" term series

with $J = K + 1$, K, and $K - 1$ respectively. Note that levels $F_{v2}(o)$, $F_{v3}(o)$, and $F_{v3}(1)$ do not exist because of the requirement that $J \geq \Omega = |\Lambda + \Sigma|$ for Hund's case "a." The B_v, D_v, and Y_v values for each vibrational level are given in Table A-3. Since Λ type doubling is small except for very large K, it has been neglected in the above formulas.

The vibrational term $G_o(v)$ is also listed in Table A-3. $H_{J''}$ for the first positive system is given by

$$H_{J''} = \frac{8}{9} \frac{\pi^2 L_o}{hc} \nu |R_e|^2 q(v', v'') \times \begin{cases} 2/3 \text{ if } K'' \text{ even} \\ 4/3 \text{ if } K'' \text{ odd} \end{cases} \times S_{K''}$$

$$3S_{K''} = S_{J''}$$

4.8 THE N_2 C $^3\Pi_u$ – B $^3\Pi_g$ (SECOND POSITIVE) SYSTEM

4.8.1 General

The structure of $^3\Pi$-$^3\Pi$ bands is simple if both states belong either to Hund's case "a" or to Hund's case "b." If both $^3\Pi$ states belong to case "a," the selection rule $\Delta\Sigma = 0$ allows division into three sub-bands: $^3\Pi_o$-$^3\Pi_o$, $^3\Pi_1$-$^3\Pi_1$, and $^3\Pi_2$-$^3\Pi_2$. Should Λ type doubling be disregarded, each sub-band has a strong R, a strong P, and (except for $^3\Pi_o$-$^3\Pi_o$) a weak Q branch. If both $^3\Pi$ states belong to case "b" or if both go over from case "a" to case "b" with increasing rotation, the same six strong bands occur. For all values of K in case "a," and for large values of K in case "b," the three P branches are close together and the three R branches are close together, giving rise to a characteristic triplet structure.

4.8.2 Line Frequencies

In the N_2 second positive system, both $^3\Pi$ states belong to case "a" for small K values. Both go over to case "b" for large values of K. Figure 4-5 shows the six

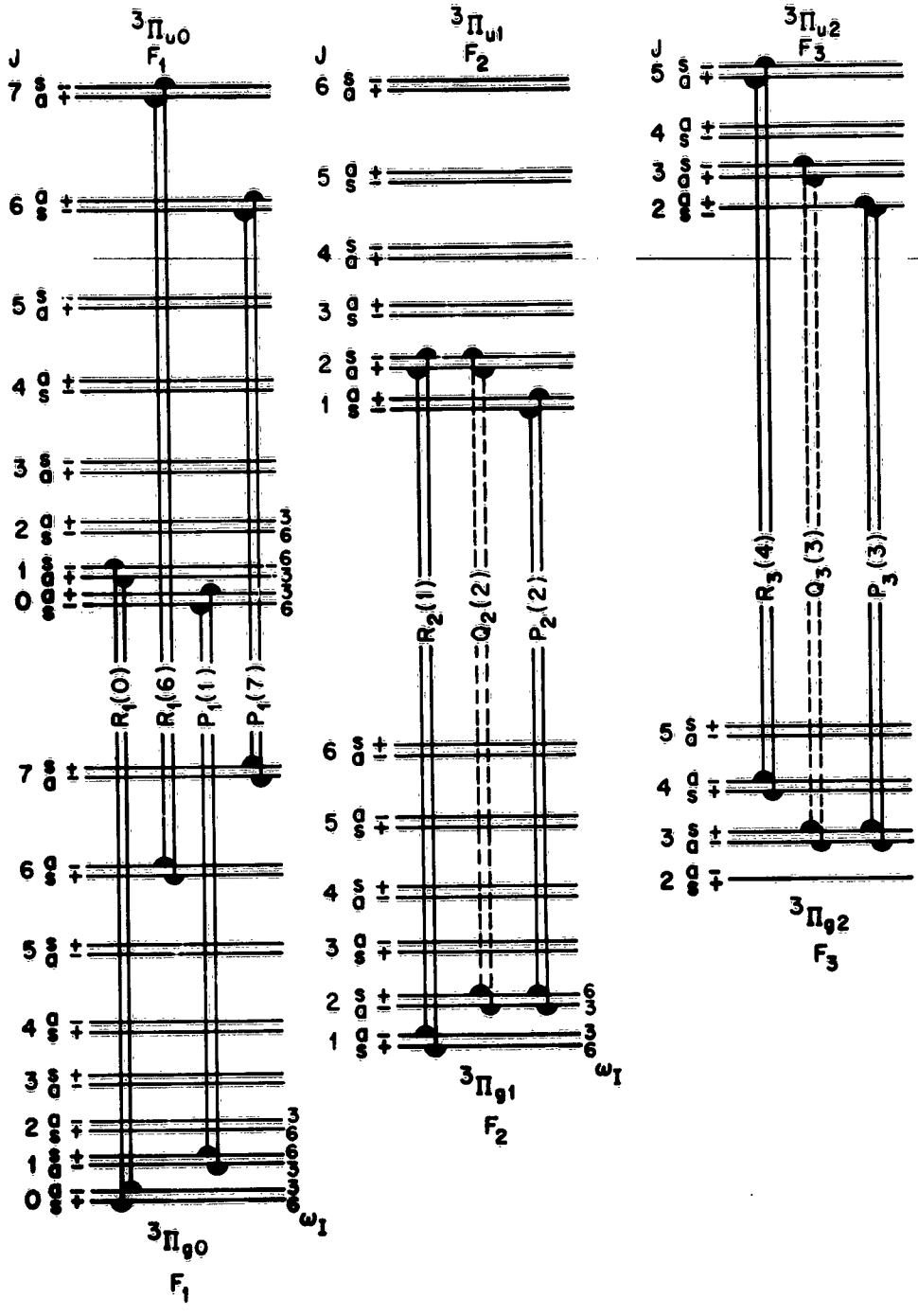

Fig. 4-5 C $^3\Pi_u$ - B $^3\Pi_g$ Band of N_2 (2nd Positive System)

main branches of the $C\,^3\Pi_u$-$B\,^3\Pi_g$ system and the corresponding energy level diagram. A rapid transition from case "a" to case "b" has been assumed. Note that both states are "regular," i.e., $^3\Pi_0 < {}^3\Pi_1 < {}^3\Pi_2$. The Λ-type doubling shown in the figure is greatly exaggerated. (Λ-type doubling will be neglected in this study; the formulas for the rotational terms F_1, F_2, and F_3 should not be affected other than trivially.) A few of the levels are labeled with the associated nuclear spin statistical weight, which is written to the right of the level. Since nitrogen nuclei follow Bose statistics ($I = 1$), the symmetrical levels (s) will have the higher statistical weight $\omega_I(s) = (2I + 1)(I + 1)$, and the antisymmetrical levels (a) will have the lower statistical weight $\omega_I(a) = (2I + 1)\,I$; i.e., $\omega_I(s) = 6$ and $\omega_I(a) = 3$. Therefore the total weight for the Λ doublet is $\omega_I = 9$, which is just $\frac{1}{2}$ of the "maximum" weight $\omega_\Omega(2I + 1)^2 = 18$ that one would expect for a heteronuclear system of the same type and for which both nuclei have $I_a = I_b = 1$.

The lines indicated in the figure are in agreement with the selection rules $+ \longleftrightarrow -$, $s \longleftrightarrow s$, $a \longleftrightarrow a$, and $J = 0, \pm 1$; except that $\Delta J = 0$ is forbidden for $\Omega = 0 \rightarrow \Omega = 0$. (There can be no Q branch for $^3\Pi_0$-$^3\Pi_0$.) The Q_2 and Q_3 branches have line intensities that fall off as $1/J^n$, and hence the total intensity residing in these branches is small. Therefore, these branches will be omitted in the present study. Finally, we note that the line $P_1(o)$ is missing in $^3\Pi_0$-$^3\Pi_0$, the lines $P_2(o)$, $P_2(1)$, and $R_2(o)$ in $^3\Pi_1$-$^3\Pi_1$, and the lines $P_3(o)$, $P_3(1)$, $P_3(2)$, $R_3(o)$, and $R_3(1)$ in $^3\Pi_2$-$^3\Pi_1$ in conformity with the rule that $J \geq \Omega$.

Formulas for the rotational terms F_1, F_2, and F_3 have been given by Budó (Ref. 10):

$$F_1(J) = B_v\left[J(J+1) - \sqrt{z_1} - \frac{2}{3}\frac{z_2}{z_1}\right] - D_v\left(J - \frac{1}{2}\right)^4 \qquad (J \geq o)$$

$$F_2(J) = B_v\left[J(J+1) + \frac{4}{3}\frac{z_2}{z_1}\right] - D_v\left(J + \frac{1}{2}\right)^4 \qquad (J \geq 1)$$

$$F_3(J) = B_v\left[J(J+1) + \sqrt{z_1} - \frac{2}{3}\frac{z_2}{z_1}\right] - D_v(J + 3/2)^4 \qquad (J \geq 2)$$

where

$$z_1 = \Lambda^2 Y_v(Y_v - 4) + \frac{4}{3} + 4J(J+1)$$

$$z_2 = \Lambda Y_v(Y_v - 1) - \frac{4}{9} - 2J(J+1) \quad ,$$

and $Y = A_v / B_v$ is a measure of the strength of coupling of the spin to the internuclear axis.

If $\nu_{v'',v'} = \nu_{oo} + G'_o(v') - G''_o(v'')$, then the frequencies of the lines will be given by

$$\overset{R_n}{\nu}_{J''} = \nu_{v'',v',J''(J''+1)} = \nu_{v'',v'} + F'_n(J''+1) - F''_n(J'')$$

and

$$\overset{P_n}{\nu}_{J''} = \nu_{v'',v',J''(J''-1)} = \nu_{v'',v'} + F'_n(J''-1) - F''_n(J'')$$

for $n = 1, 2, 3$. Again, Λ type doubling is neglected.

4.8.3 Line Intensities

The two lines arising from the components of a Λ type doublet overlap in frequency and are identical except for the ω_I , one having the value 6 (symmetric) and the other 3 (antisymmetric). This allows us to construct the $H_{n'',n',v'',v',J'',J'} = H_{J'',J'}$ for the whole doublet by simply adding the H's for the individual components, viz:

$$H_{J'',J'} = \frac{8\pi^2 L_o}{3hc} \cdot \frac{1}{2 \cdot 3} \cdot \nu_{J'',J'} |R_e|^2 \, q(v',v'') \, S_{J''} \left[\frac{3}{9/2} + \frac{6}{9/2}\right]$$

$$= \frac{8\pi^2 L_o}{9hc} \nu_{J'',J'} |R_e|^2 \, q(v',v'') \, S_{J''}$$

where $9/2$ is the value of Q_{nuclear}.

Hönl-London factors for $^3\Pi$-$^3\Pi$ systems under various coupling conditions have been given by Budó (Ref. 12). For this study it will be sufficiently accurate to use the Hönl-London factors for a $^1\Pi$-$^1\Pi$ type transition:

$$S^{\bar{R}}_{J''} = J'' + 1$$

$$S^{\bar{P}}_{J''} = J'' \quad .$$

The final formulas for $H_{n'',n',v'',v',J'',J'}$ then become

$$H^{\bar{R}_n}_{J''} = \frac{8\pi^2}{9hc} \bar{L}_o \, \nu^{\bar{R}_n}_{J''} \, |\bar{R}_e|^2 \, q(v',v'') \, [J'' + 1]$$

and

$$H^{\bar{P}_n}_{J''} = \frac{8\pi^2}{9hc} \bar{L}_o \, \nu^{\bar{P}_n}_{J''} \, |\bar{R}_e|^2 \, q(v',v'') \, J''$$

for $n = 1, 2, 3$. Finally,

$$E_{v'',J''} = \frac{hc}{k} \left[G''_o(v'') + F''_n(J'') \right] \quad n = 1, 2, 3$$

4.8.4 Molecular Constants

The molecular constants for the $C\,^3\Pi_u$ and $B\,^3\Pi_g$ states of N_2 which were used in this study are given in Table A-3. The values of B_v, D_v, and Y_v are due to Budó. The vibrational terms $G_o(v)$ were taken from Coster, Brons, and Van der Ziel (Ref. 13).

The quantity F_{max} listed in Table A-3 gives the maximum value that any of the rotational terms $F_{v,n}$ $(n = 1, 2, 3)$ may have. The rotational formulas are probably not accurate beyond $J = 50$ or 60. The extent to which they fail is not known, but it is felt not to be great until about $J = 80$.

Table A-4b shows the bands included in the present calculation along with the Franck-Condon factors used. Note that the vibrational levels in the upper state stop at $v' = 4$. The potential curve does not break off at $v' = 4$ however, and although transitions from $v' > 4$ have not been observed, one should in a local thermodynamic equilibrium situation go to $v' > 4$. Franck-Condon factors and B' values are not known for $v' > 4$, but the B's could be obtained by extrapolation.

4.9 THE $B\,^2\Sigma_u^+ - X\,^2\Sigma_g^+$ (FIRST NEGATIVE) SYSTEM OF N_2^+

4.9.1 General

Since $^2\Sigma$ states always belong strictly to Hund's coupling case "b," giving rise to the selection rule $\Delta K = \pm 1$ with $\Delta K = 0$ being forbidden, the structure of a $^2\Sigma - ^2\Sigma$ transition is simple. There are two principal branches, an R branch and a P branch, each of which may be resolved into three components according to the rule $\Delta J = 0, \pm 1$. For one of these ($\Delta J = 0$) $\Delta J \neq \Delta K$.

4.9.2 Line Frequencies

The energy level diagram and transitions which apply to first negative bands are shown in Fig. 4-6. Rotation terms of lower $^2\Sigma_g^+$ and upper $^2\Sigma_u^+$ states are both given by

$$F_v(K) = B_v K(K + 1) - D_v K^2(K + 1)^2$$

where the spin splitting of each rotational level is ignored. Table A-5 lists the values of B_v, D_v, and $G_0(v)$ used in the calculation. The included bands and corresponding Franck-Condon factors are given in Table A-6. Bands with very small F-C factors have been omitted.

The lines and their corresponding Hönl-London factors are given in Table A-2.

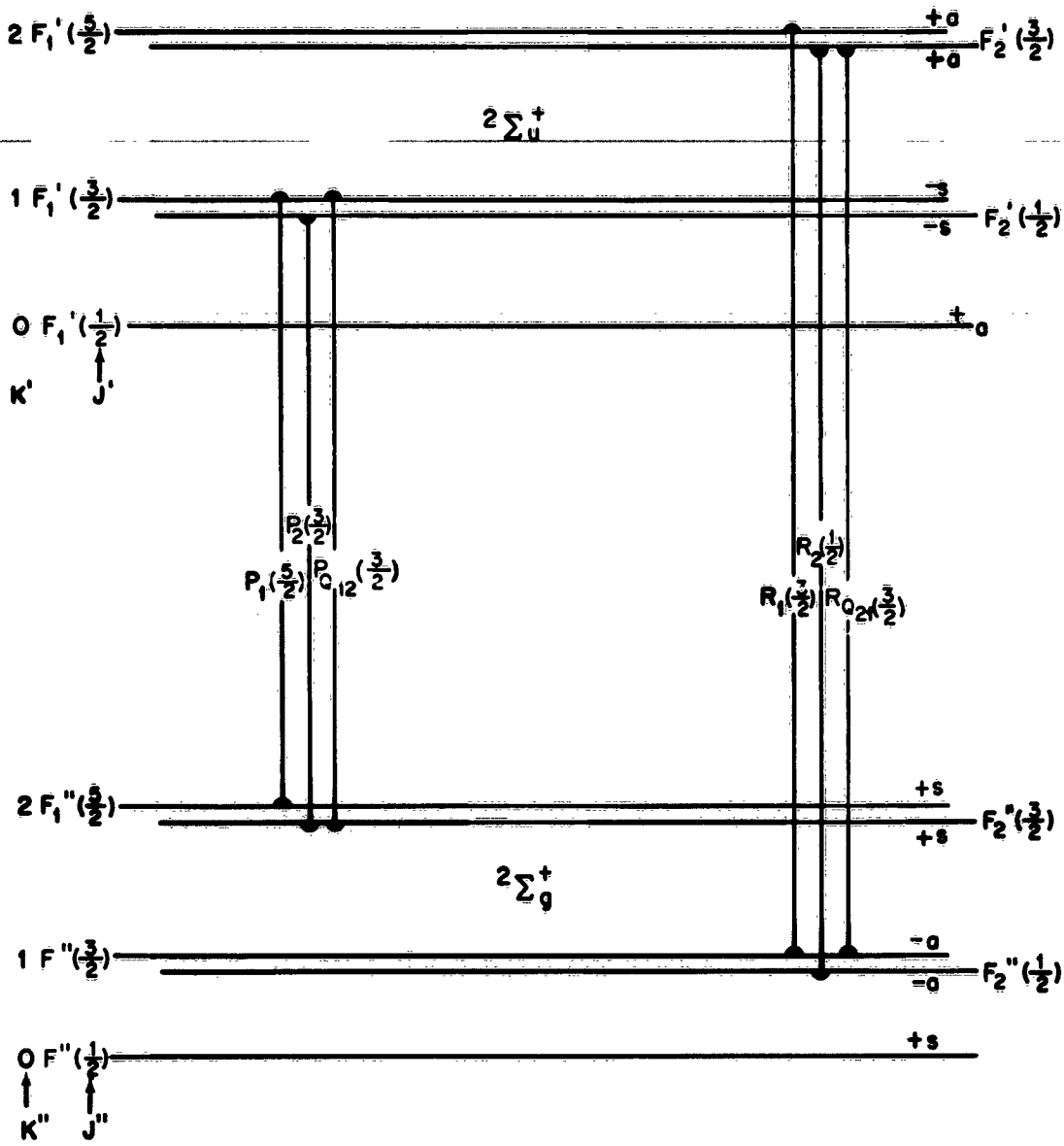

Fig. 4-6 $B\ ^2\Sigma_u^+ - X\ ^2\Sigma_g^+$ Band of N_2^+ (1st Negative System)

4.9.3 Line Intensities

Grouping together P_1, P_2, and $^{P}Q_{12}$ into a single line, the sum of the S_J's is $2K''$. For the group R_1, R_2, and $^{R}Q_{21}$, the sum of the strength factors is $2(K'' + 1)$. Ignoring the spin, the rotational levels can be labeled by K. The $H_{J'',J'}$'s are:

$$H_{J'',J'} = \frac{16\pi^2}{3hc} \nu_{K'',K} |R_e|^2 q(v',v'') S_{K''} \cdot \begin{cases} 2/3 \text{ if } K'' \text{ even} \\ 1/3 \text{ if } K'' \text{ odd} \end{cases}$$

where

$$S''_K = K'' + 1 \text{ if } K' = K'' + 1$$
$$= K'' \quad \text{if } K' = K'' - 1$$

The factors to allow for K odd or even arise because of the effect of symmetry properties on $^2\Sigma$-$^2\Sigma$ transitions of homonuclear molecules. Even K'' levels are symmetric ($\omega_I(s) = 6$), while odd K'' levels are antisymmetric ($\omega_I(s) = 3$).

4.10 THE $B\,^2\Pi - X\,^2\Pi$ (BETA) SYSTEM OF NO

4.10.1 General

The structure of a $^2\Pi$-$^2\Pi$ system is simple if both states belong to Hund's coupling case "a" or both belong to case "b" or if, as in the present case, both states are intermediate between cases "a" and "b" and go over together from case "a" to case "b" with increasing nuclear rotation. There are two sub-bands in the NO Beta system: $^2\Pi_{1/2}$-$^2\Pi_{1/2}$ and $^2\Pi_{3/2}$-$^2\Pi_{3/2}$. Each sub-band consists of a strong R, a strong P, and weak Q branch.* Both the B and X states are regular, that is, $^2\Pi_{1/2} < {}^2\Pi_{3/2}$. Since the intensity of the Q branches falls off like J^{-1}, we will neglect these branches entirely.

*See Fig. 4-7.

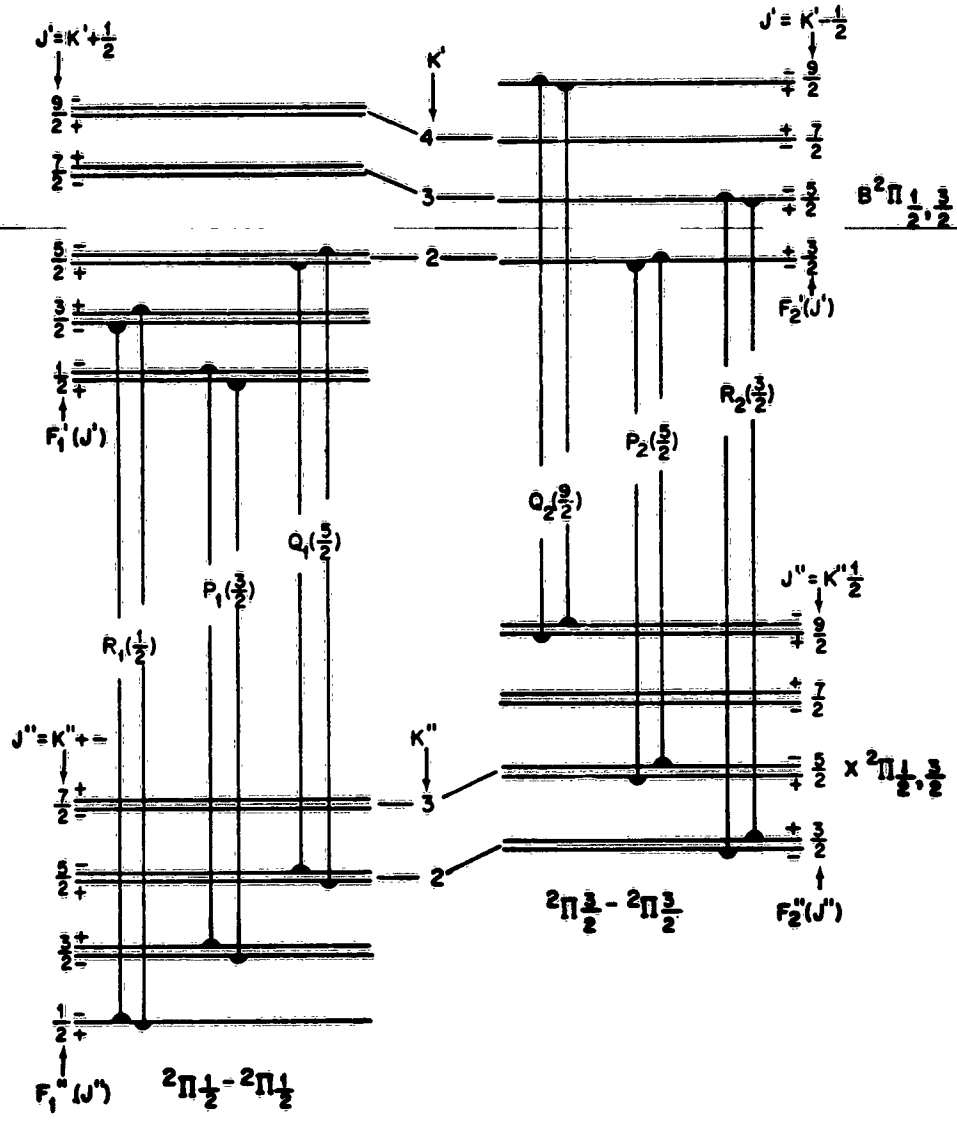

Fig. 4-7 B $^2\Pi$ - X $^2\Pi$ Band of NO (β System)

4.10.2 Line Frequencies

Both the $B\ ^2\Pi$ and $X\ ^2\Pi$ states of NO are intermediate between Hund's coupling cases "a" and "b," with the X state being nearer case "a" ($A = 124.2\ cm^{-1}$) than the B state (for which $A \sim 32\ cm^{-1}$). A general formula for the term values of a $^2\Pi$ state with coupling intermediate between cases "a" and "b" has been derived by Hill and Van Vleck (Ref. 14):

$$T_n(v,J) = T_e + G_n(v) + B_v\left[\left(J + \frac{1}{2}\right)^2 - 1 + (-1)^n \mu(J)\right] - D_v \begin{cases} J^4 & (n = 1) \\ (J+1)^4 & (n = 2) \end{cases}$$

where

$$\mu(J) = \sqrt{\left(J + \frac{1}{2}\right)^2 - Y_v + Y_v^2/4} \quad \text{and} \quad Y_v = A/B_v$$

Here the subscript $n = 1$ stands for a $^2\Pi_{1/2}$ and $n = 2$ stands for $^2\Pi_{3/2}$. A subscript n has been affixed to the vibrational term G(v), since the different substates of the multiplet may have slightly different vibrational levels. Formulas for the line frequencies of the two R and two P branches follow.

$$R_1(J) = \nu_e + \nu_v^{(1)} + F_1'(J'' + 1) - F_1''(J'')$$

$$R_2(J) = \nu_e + \nu_v^{(2)} + F_2'(J'' + 1) - F_2''(J'')$$

$$P_1(J) = \nu_e + \nu_v^{(1)} + F_1'(J'' - 1) - F_1''(J'')$$

$$P_2(J) = \nu_e + \nu_v^{(2)} + F_2'(J'' - 1) - F_2''(J'')$$

where

$$\nu_e = T_e' - T_e''$$

$$\nu_v^{(n)} = \nu_{v'',v'}^{(n)} = G_n'(v') - G_n''(v'') \quad , \quad n = 1, 2$$

and

$$F_n(J) = F_n(v,J) = B_v \left\{ \left(J + \frac{1}{2}\right)^2 - 1 + (-1)^n \left[\left(J + \frac{1}{2}\right)^2 - Y_v + Y_v^2/4 \right]^{1/2} \right\}$$

$$- D_v \cdot \begin{cases} J^4 & n = 1 \\ (J+1)^4 & n = 2 \end{cases}$$

with B_v, D_v, $G_1(v)$, and $G_2(v)$ being given in Table A-7.

4.10.3 Line Intensities

As the $^2\Pi$ states approach case "b," the selection rule $\Delta K = 0, \pm 1$ holds. Also branches with $\Delta K \neq \Delta J$ are very weak. Disregarding Λ type doubling and neglecting the weak Q branches and satellite branches, the band structure is similar to that of a $^2\Sigma$-$^2\Sigma$ transition, i.e., 4 strong branches. Intensity factors for case "a" and case "b" coupling are given in Table A-2. If the satellite lines are considered as part of a composite lines, but Q branches are still ignored, the intensity factors may be given with sufficient accuracy for our purpose by:

$$S_{J''}^{R_2} = S_{J''}^{R_1} = J'' + 1$$

$$S_{J''}^{P_2} = S_{J''}^{P_1} = J''$$

and the H factors are then

$$H_{J''} = \frac{4\pi^2 L_o}{3hc} |R_e|^2 \nu_{J'',J'} q(v',v'') S_{J''}$$

The Franck-Condon factors $q(v',v'')$ are presented in Table A-8a.

4.11 THE $A\,^2\Sigma - X\,^2\Pi$ (GAMMA) SYSTEM OF NO

4.11.1 General

The $X\,^2\Pi$ state of NO belongs neither strictly to coupling case "a" nor to case "b," but to a transition case which goes from case "a" to case "b" with increasing rotation. However, the $A\,^2\Sigma$ state belongs strictly to case "b," and as a result of this combination the structure of the NO gamma bands is quite complicated. The $^2\Pi$ state has been discussed previously (see NO Beta system). Figure 4-8 shows levels and transitions applicable to the NO gamma system.

4.11.2 Line Frequencies

The general term formula is given in the preceding discussion of the NO Beta system. B_v, D_v, Y_v, $G_o^{(1)}(v)$, and $G_o^{(2)}(v)$ for the $X\,^2\Pi$ state are presented in Table A-7, as are B_v, D_v, and $G_o(v)$ for the $A\,^2\Sigma$ state. The quantum number K has been formally extended to levels having small rotation in the case of the $A\,^2\Sigma$ state (Ref. 5). Rotational terms for this state are given by:

$$F_v(K) = B_v K(K+1) - D_v K^2(K+1)^2$$

4.11.3 Line Intensities

Intensity factors for the twelve branches are given (apart from an arbitrary constant) by Earls (Ref. 15). These formulas were normalized to obey the sum rule. The resulting expressions are given in Table A-2. After combining branches and satellites and omitting two weak transitions, 6 composite lines serve the needs of our calculation. Intensity factors for these lines are also given in Table A-2.

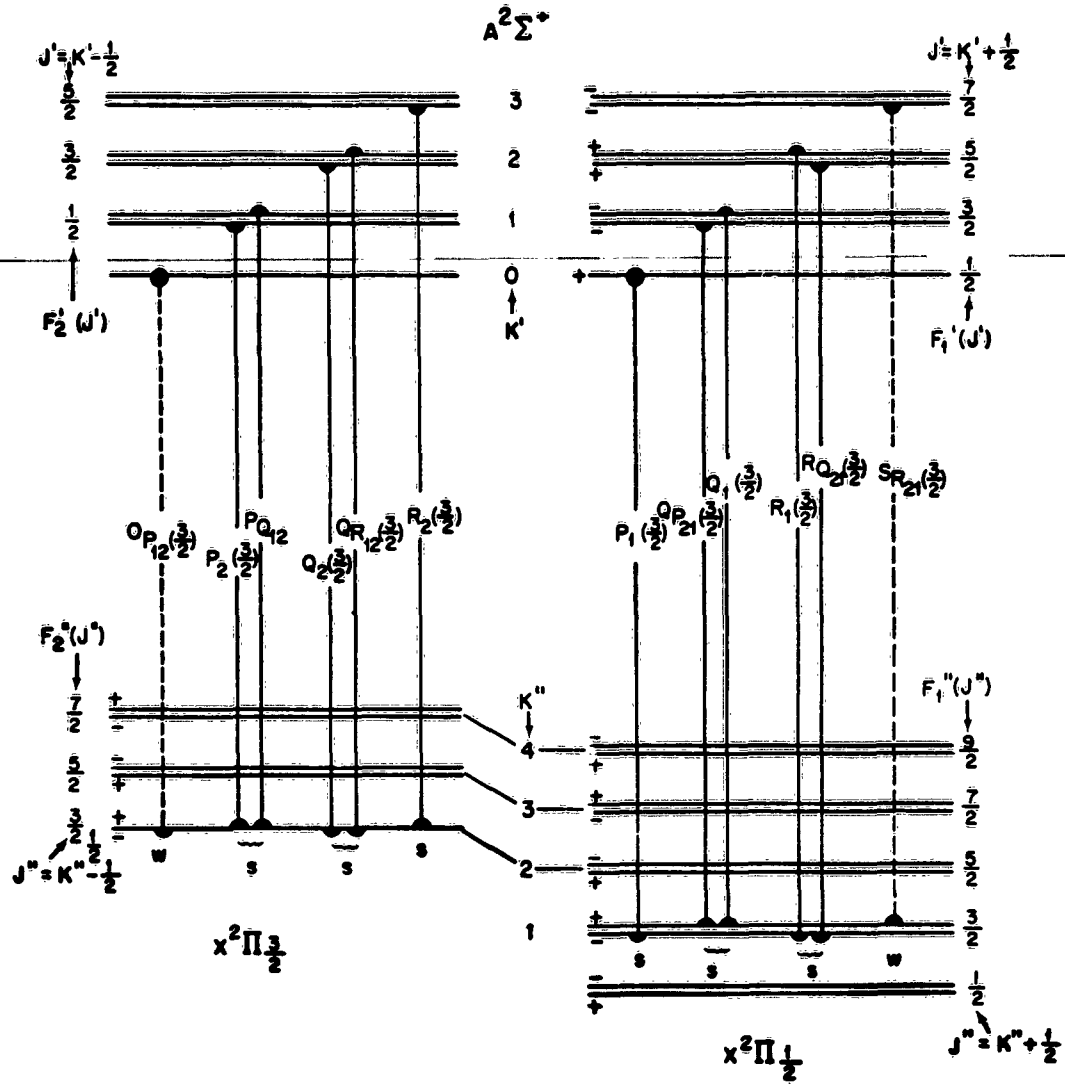

Fig. 4-8 $A\,^2\Sigma - X\,^2\Sigma$ Band of NO (γ System)

The $H_{J'',J'}$'s for the NO Gamma system are then:

$$H_{J'',J'} = \frac{2\pi^2 L_o}{3hc} \nu_{J'',J'} |R_e|^2 q(v',v'') S^*_{J''}$$

where the $S^*_{J''}$ are the composite intensity factors described above. The Franck-Condon factors $q(v',v'')$ for the transitions are listed in Table A-8b.

Section 5
THE SACHA* CODES

5.1 MAGNETIC-TAPE LINE ATLASES

Digital computer codes (for the IBM 7090) have been constructed to write the magnetic-tape line atlases for the six molecular systems to be included in the calculation. For each system, the spectral lines and their "H" and "E" functions [see Eqs. (3.21) and (3.22) and Subsections 4.6 to 4.11] are generated according to vibrational and rotational quantum numbers and labeled by an identification vector. These lines are then merged and sorted according to line frequency. For each spectral line, there are three decimal numbers and one octal number (the identification vector) on tape:

ν	α	H_α	E_α
(frequency)	(identification vector)		

where α is formed of the upper and lower vibrational and rotational quantum numbers, the branch number, and an integer from 1 to 6 which specifies the molecular system to which the line belongs.

The systems, their "key" integer η, and the total number of lines stored on tape for each system are:

$\eta = 1$	O_2	Schumann-Runge	13,836
2	N_2	First Positive	58,476
3	N_2	Second Positive	16,750
4	N_2^+	First Negative	21,306
5	NO	Beta	15,760
6	NO	Gamma	25,400
		Total Lines	151,528

*Spectral Absorption Coefficient of Heated Air.

In addition to the individual system line atlases, a tape consisting of all the systems merged according to frequency has been written. This merged tape containing all 151,528 lines will serve as the spectral line atlas for air. By masking techniques, the origin of each line may be found from its identification vector, i.e., its species, lower level, etc. To compute the absorption coefficient, the atlas tapes must be used in conjunction with population numbers and partition functions corresponding to the desired air temperature and density. Population factors may be obtained by interpolating in the tables of Gilmore (Ref. 16). The vibration-rotation partition functions are given, with sufficient accuracy for our problem, in Table A-1c.

All of the Franck-Condon factors used in the atlas construction are from R. W. Nicholls (Refs. 17-19). The electronic f-values were taken from Treanor and Wurster (Ref. 20-O_2 Schumann-Runge), Bennett and Dalby (Ref. 21-N_2^+ First Negative), and Keck et al. (Ref. 21-remaining band systems).

5.2 AN AVERAGE TRANSMISSION CALCULATION

As a first effort to assay the value of the method, a code was written to calculate the average transmission of optical radiation through an isothermal, homogeneous slab of pure molecular oxygen as a function of distance through the slab. Variable parameters in the calculation are the slab temperature T, the line half-width σ, basic frequency intervals, and the number of frequency points on the line wings. The average transmission at average frequency $\bar{\nu}$ is given by

$$\bar{T}_{\Delta\nu}(\bar{\nu}, T, \sigma, N, x) = \frac{1}{\Delta\nu}\int_{\Delta\nu} \exp\left[-Nx\sum_{\alpha}\kappa_{\alpha}(\nu)\right] d\nu \qquad (5.1)$$

where $\kappa_{\alpha}(\nu)$ is the contribution per particle to the spectral absorption coefficient at frequency ν due to spectral line α, N is the particle density of O_2 molecules in the lower electronic state for the Schumann-Runge transistions, and x is the distance through the slab. The units of $\kappa_{\alpha}(\nu)$ are cm^2, those of N are cm^{-3}, and those of x are cm. $\bar{\nu}$ is the center frequency of the interval $\Delta\nu$, where ν has units cm^{-1}. When expressed in these units, the frequency is generally referred to as the "wave number." The sum runs over all lines α which contribute appreciably at ν.

The calculation was carried out by computing the average transmission as the product Nx was varied. By using this technique, the need to explicitly specify N was circumvented for these preliminary studies. The product Nx is referred to herein as the "effective depth." Since these preliminary calculations were done for temperatures at or below 5,000°K, emission was neglected.

Some representative results of the calculation are presented in figs. 5-1 through 5-5. Figures 5-1 and 5-2 demonstrate the effect of variation of the line-width parameter for fixed values of the other parameters as noted in the figures.

Average transmission is plotted versus frequency in figs. 5-3 through 5-5, for various values of $\bar{T}$, σ, and Nx. Although smooth curves have been drawn, the calculation was carried out only for isolated frequency intervals of 100 cm^{-1} width. These intervals were centered at ten frequency points from 31,500 cm^{-1} to 49,500 cm^{-1}, the difference between points being 2,000 cm^{-1}.

When only one molecular species is involved, the relation between particle and linear absorption coefficients is

$$\mu(\nu) = N\kappa(\nu) \qquad (5.2)$$

where $\mu(\nu)$ has the usual units cm^{-1}.

5.3 COMPARISON OF RESULTS

An earlier calculation carried out at this laboratory by Meyerott, Sokoloff, and Nicholls (Ref. 1) affords the only known results which are comparable with those of the present work. In the earlier calculation (hereafter referred to as the MSN paper), the average discrete absorption coefficient was computed over a much wider frequency range, using basic averaging intervals of 0.25 ev (roughly 2,000 cm^{-1}). Computation was carried out by desk calculator and included a large number of vibrational bands for each of the six molecular transitions needed for the air absorption calculation. Rotational structure was not included, with the total band contribution taken at band head energy.

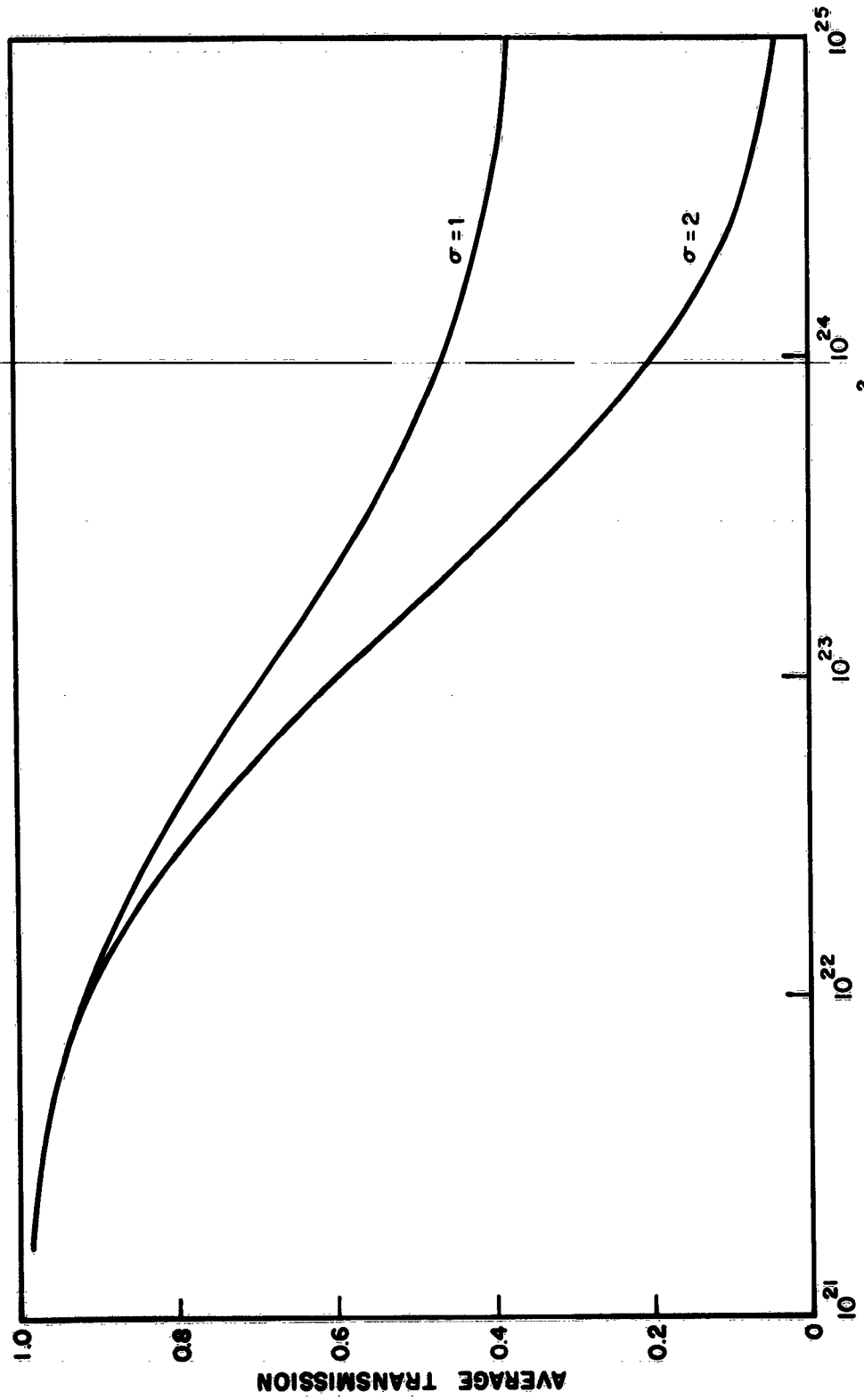

Fig. 5-1 Effect of Half-Width Variation on Optical Properties of O_2 for ν = 31500 cm^{-1} and T = 2000°K

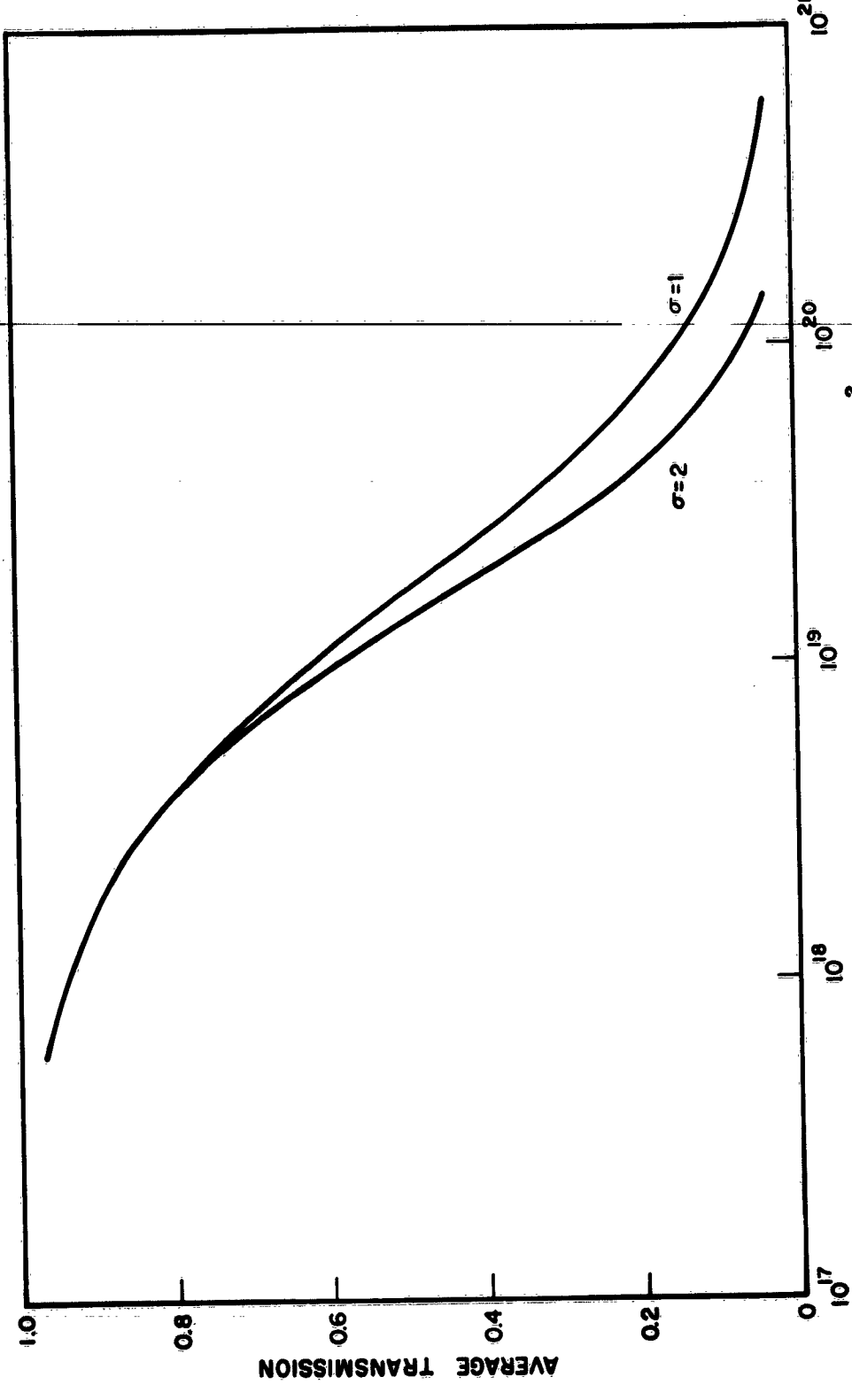

Fig. 5-2 Effect of Half-Width Variation on Optical Properties of O_2 for ν = 47500 cm^{-1} and T = 2000°K

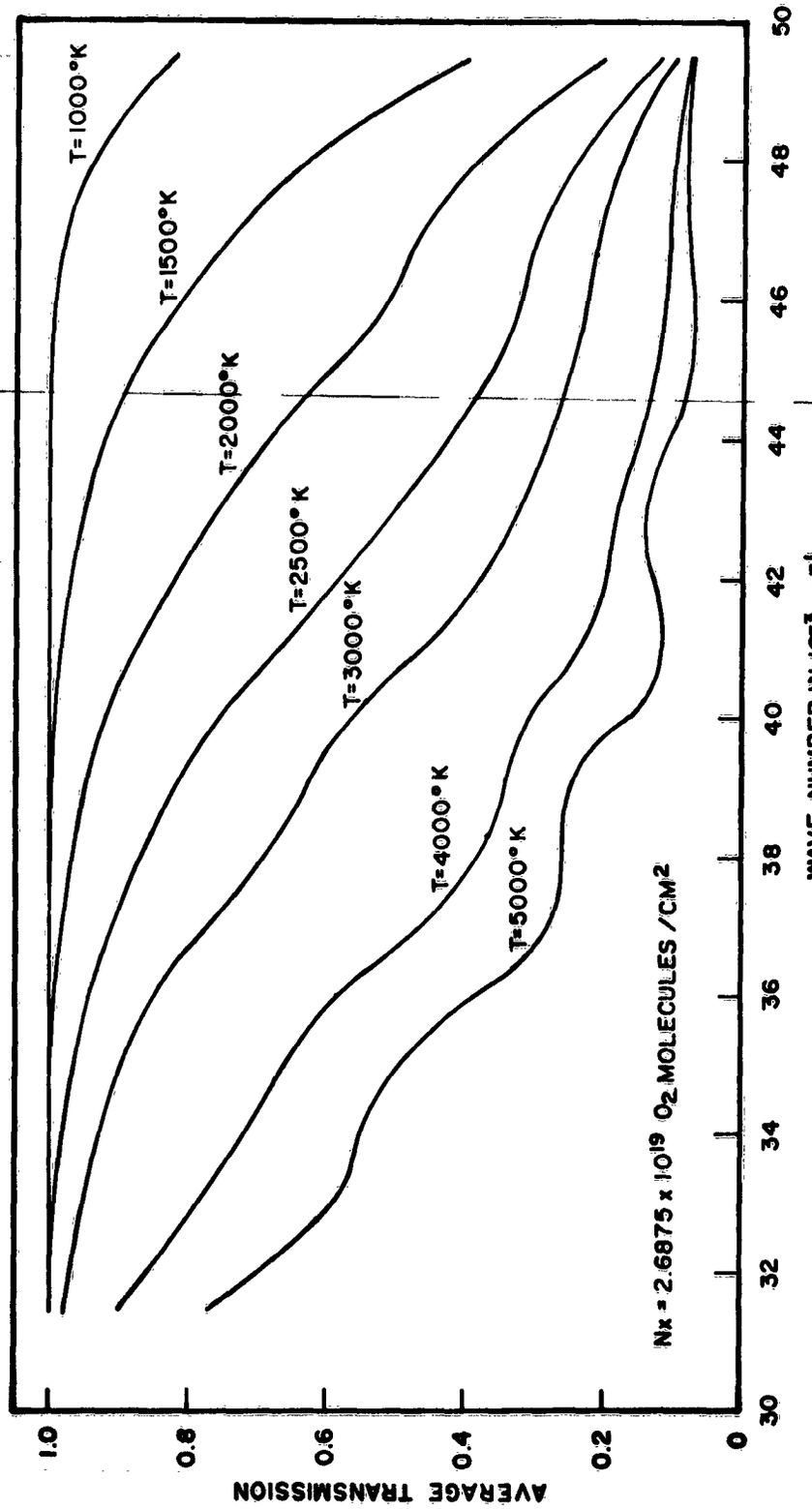

Fig. 5-3 SACHA Code Average Transmission Result for O_2 ($\sigma = 0.75$)

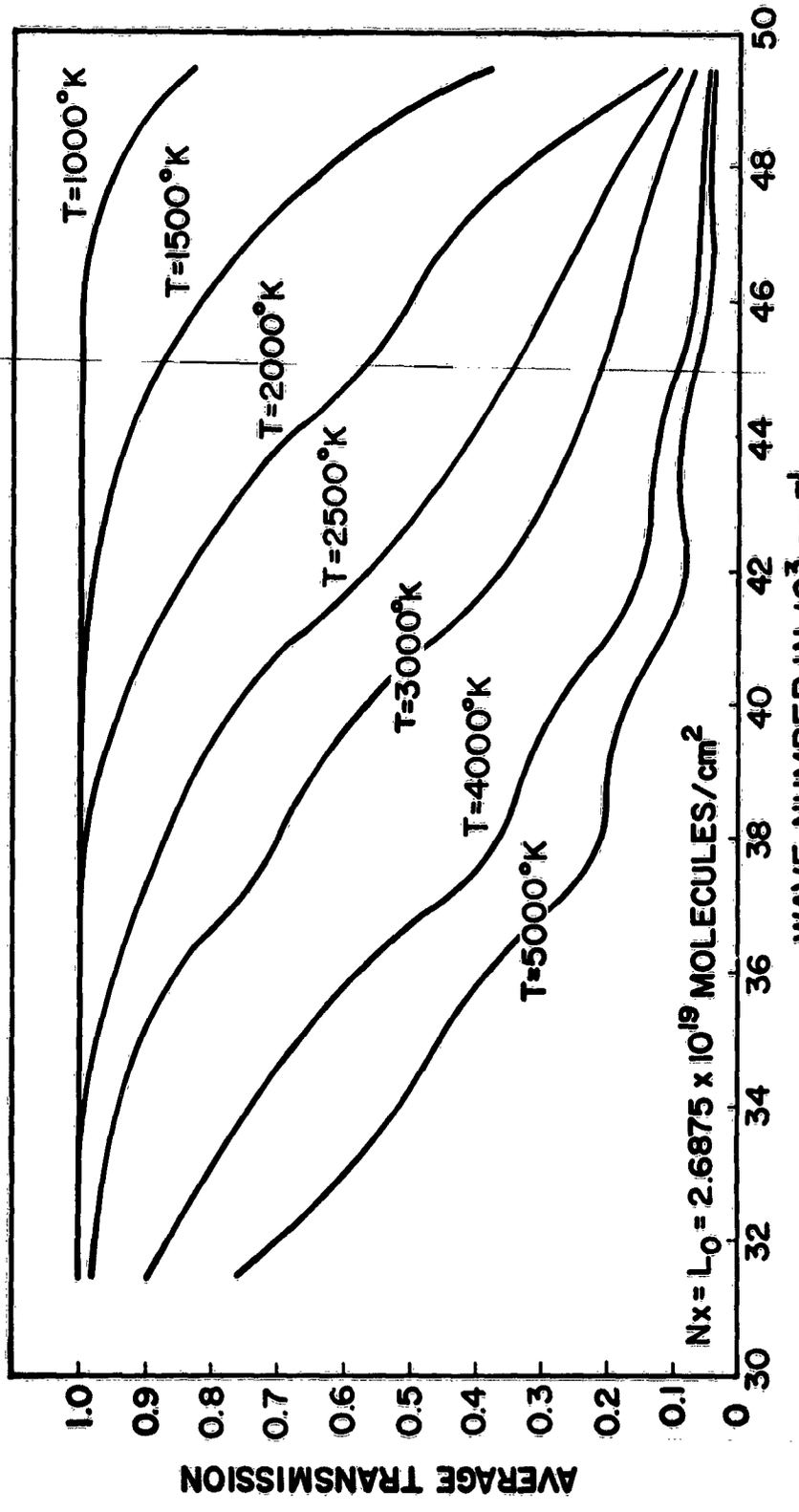

Fig. 5-4 SACHA Code Average Transmission Results for O_2 (σ = 1.0)

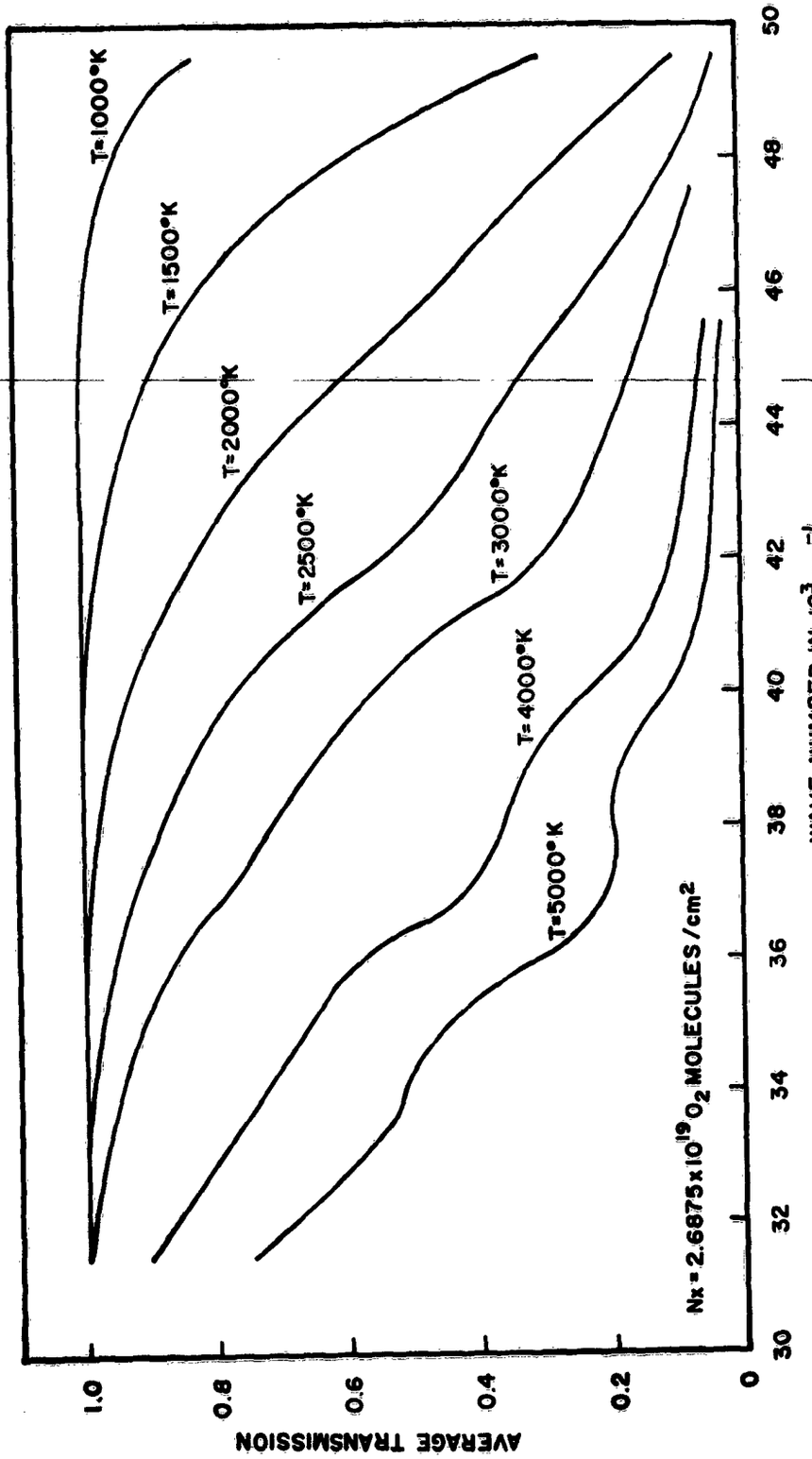

Fig. 5-5 SACHA Code Average Transmission Results for O_2 (σ = 2.0)

Since this work was published previous to the availability of many of the O_2 Schumann-Runge Franck-Condon factors, these had to be estimated.

Figure 5-6 was prepared by calculating average transmissions, utilizing the O_2 Schumann-Runge absorption coefficients listed in the MSN paper, after modification of the electronic f-number and level population to agree with those assumed in the present work.

The cause for the differences between the two calculations has not been extensively investigated. Apart from the large difference between basic frequency intervals employed in the averaging process, the major contribution to the discrepancy appears to arise from the omission of several important band systems in the previous work.

Inclusion of many more bands, consideration of rotational structure, and smaller frequency intervals for averaging are among the factors giving rise to the more smoothly varying transmission obtained in the SACHA results. More Franck-Condon factors were available for the present study, and better values had replaced some of those used in the earlier calculations.

5.4 A CALCULATION FOR HEATED AIR

Another machine program in the SACHA series is nearing completion. This code will compute the average transmission of optical radiation through a slab of heated air. Mean absorption coefficients will also be obtained over the frequency range of interest. The six molecular transitions discussed in this report will be included in the calculation, with the species concentration and fractional population for the lower electronic state of the transition being obtained by interpolation in Gilmore's Tables. At a later date provision may also be made to include the continuum contribution to the absorption coefficient. Transmissions and absorption coefficients will also be obtained for the individual constituents of air.

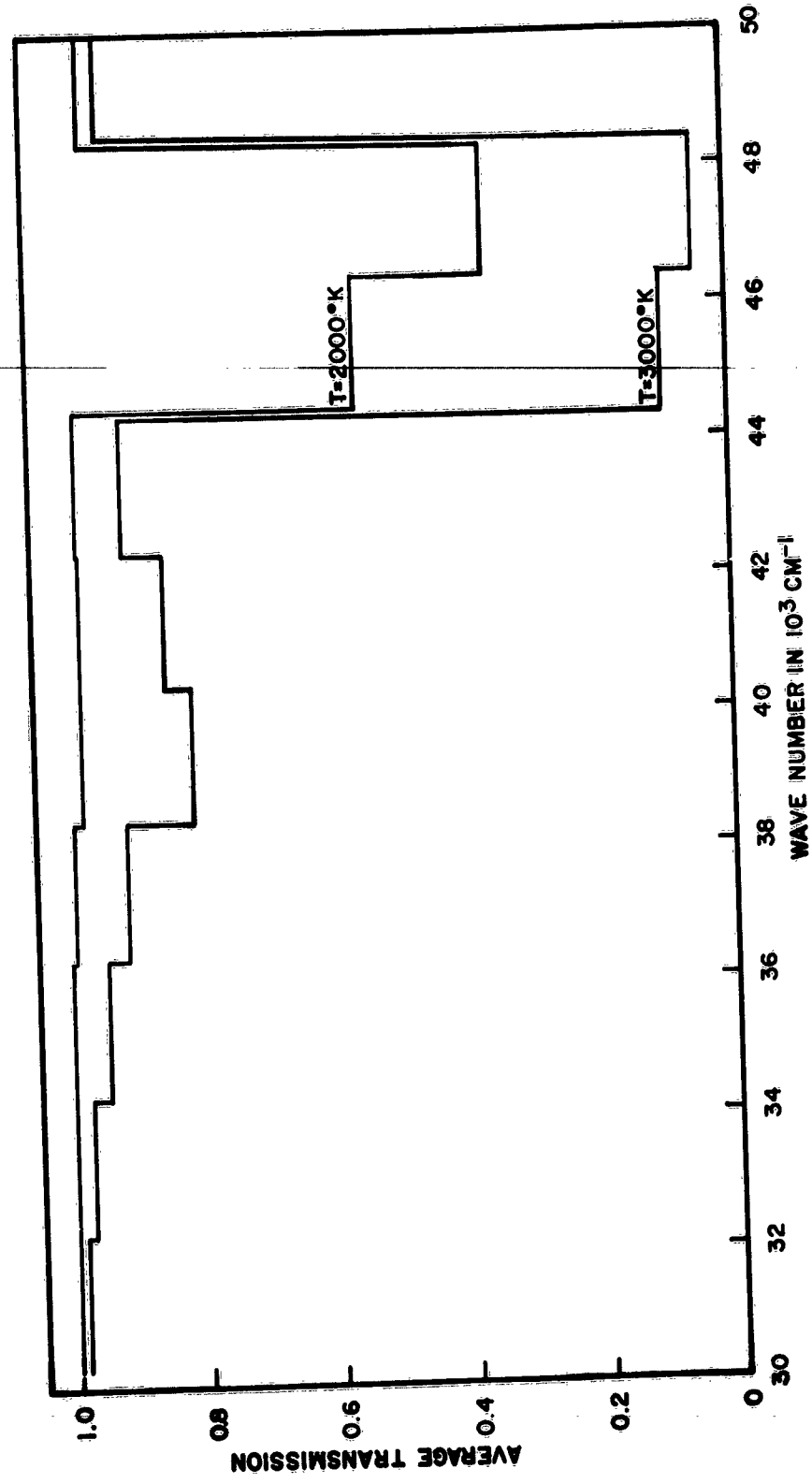

Fig. 5-6 Average Transmission Through 1 cm of O_2 (calculated from results of Meyerott, Sokoloff, and Nicholls, 1959). Electronic f-number and populations normalized to agree with SACHA results.

Section 6
REFERENCES

1. Air Force Cambridge Research Center, Absorption Coefficients of Air, by R. E. Meyerott, J. Sokoloff and R. W. Nicholls, Geophysics Research Paper No. 68, Bedford, Mass., 1960
2. Air Force Special Weapons Center, Radiative Properties of High Temperature Gases, by B. H. Armstrong, D. E. Buttrey, L. Sartori, A. J. F. Siegert and J. D. Weisner, AFSWC TR 61-72, Vol. 1, October 1961
3. B. H. Armstrong, J. Sokoloff, R. W. Nicholls, D. H. Holland and R. E. Meyerott, "Radiative Properties of High Temperature Air," J. Quant. Spectrosc. Radiat. Transfer, Vol. 1, 1961, p. 143, ff.
4. V. A. Ambartsumyan, Theoretical Astrophysics, Pergamon Press, New York, 1958
5. G. Herzberg, Spectra of Diatomic Molecules, Van Nostrand, New York, 1950
6. H. A. Bethe, OSRD Report 369, Feb 9, 1942
7. F. Brinkerly, OSRD Report 3550, April 27, 1944
8. W. Jevons, Report on Band Spectra of Diatomic Molecules, Physical Society of London, 1932
9. R. Schlapp, "Fine Structure in the $^3\Sigma$ Ground-State of the Oxygen Molecule, and the Rotational Intensity Distribution in the Atmospheric Oxygen Band," Phys. Rev., Vol. 51, 1937, p. 342
10. A. Budó, "Uber die Triplett - Bandentermformel fur den Allgemeinen Intermediaren Fall und Anwendung derselben auf die $B^3\Pi$-, $C^3\Pi$-Terme des N_2 - Molekuls," Z. Physik, Vol. 96, 1935, p. 219
11. A. Budo, "Die Rotationskonstanten B, D und Y der $^3\Pi$ - Terme von TiO, C_2, CO, PH, Al H, NH," Z. Physik, Vol. 98, 1936, p. 437

12. A. Budo, "Intensitatsformeln fur die Triplettbauden, Z. Physik, Vol. 105, 1937, p. 579

13. D. Coster, F. Brons, and A. van der Ziel, "Die Sogenannte Zweite Positive Gruppe des Stickstoffspektrums, Z. Physik, Vol. 84, 1933, p. 304

14. E. Hill and J. H. Van Vleck, "On the Quantum Mechanics of the Rotational Distortion of Multiplets in Molecular Spectra," Phys. Rev., Vol. 32, 1928, p. 250

15. L. T. Earls, "Intensities in $^2\Pi - {}^2\Sigma$ Transitions in Diatomic Molecules," Phys. Rev., Vol. 48, 1935, p. 423

16. Rand Corporation, Equilibrium Composition and Thermodynamic Properties of Air to 24,000°K, by F. R. Gilmore, Research Memorandum RM-1543, Santa Monica, California, 1955

17. R. W. Nicholls, "The Franck-Condon Factor q(v', v") Array to High Vibrational Quantum Numbers for the 0_2 ($B^3\Sigma_u^- - X^3\Sigma_g^+$) Schumann-Runge Band System," Can. J. Phys., Vol. 38, 1960, p. 1705

18. R. W. Nicholls, "Franck-Condon Factors to High Vibrational Quantum Numbers: N_2 and N_2^+," J. Res. N. B. S., Vol. 65A, 1961, p. 451

19. R. W. Nicholls, "Franck-Condon Factors to High Vibrational Quantum Numbers II: SiO, MgO, AlO, VO, NO," J. Res. N.B.S, Vol. 66A, 1962, p. 227

20. C. E. Treanor and W. H. Wurster, "Measured Transition Probabilities for the Schumann-Runge System of Oxygen," J. Chem. Phys., Vol. 32, 1960, p. 758

21. R. G. Bennett and F. W. Dalby, "Experimental Determination of the Oscillator Strength of the First Negative Bands of N_2^+," J. Chem. Phys., Vol. 31, 1959, p. 434

22. J. C. Keck, J. C. Camm, B. Kovel and T. Wentink, "Radiation from Hot Air Part II. Shock Tube Study of Absolute Intensities," Ann. Phys., Vol. 7, No. 1, 1959

23. Rand Corporation, Theoretical Description of the Blast and Fireball for a Sea Level Megaton Explosion (U), by H. L. Brode, Research Memorandum RM-2248, Santa Monica, California (S)

24. R. D. Richtmyer, Difference Methods for Initial-Value Problems, Inter-science Ltd., New York

25. S. Chandrasedhar, Radiative Transfer, Dover Publications, 1960, pp. 1-12 and 289

26. J. Von Neumann & R. D. Richtmyer, J. Appl. Phys., Vol. 21, Mar 1950, p. 232

27. Air Research and Development Command, The ARDC Model Atmosphere, by A. Minzner, W. Champion, and H. L. Pond, AFCRC TR-t9-267, 1959

28. Rand Corporation, Graphs of X-Ray Absorption Coefficients for Fourteen Substances, Research Memorandum RM-2367-AEC, Santa Monica, California, 1959

29. Air Force Special Weapons Center, Thermodynamic Properties of Highly Ionized Air, by J. Hilsenrath, M. S. Green, and C. W. Beckett, AFSWC TR-56-35, April 1955

Appendix A
TABLES

Table A-1

MOLECULAR SYSTEMS CONSTANTS (GENERAL)

a

Spectroscopic Quantities

System	Transition (Absorption)	ν (cm^{-1}) of f Measurement	f	$\lvert R_e \rvert^2$
O_2 Schumann-Runge	$X\ ^3\Sigma_g^- \rightarrow B\ ^3\Sigma_u^-$	29,300	0.048	3.293×10^{-36}
N_2 First Positive	$A\ ^3\Sigma_u^+ \rightarrow B\ ^3\Pi_g$	12,500	0.02	3.34×10^{-36}
N_2 Second Positive	$B\ ^3\Pi_g \rightarrow C\ ^3\Pi_u$	32,000	0.07	4.6×10^{-36}
N_2^+ First Negative	$X\ ^2\Sigma_g^+ \rightarrow B\ ^2\Sigma_u^+$	25,500	0.0348	2.85×10^{-36}
NO Beta	$X\ ^2\Pi \rightarrow B\ ^2\Pi$	23,800	0.008	0.7×10^{-36}
NO Gamma	$X\ ^2\Pi \rightarrow A\ ^2\Sigma$	38,500	0.0025	0.14×10^{-36}

b

Statistical Quantities

Molecule and State	I_a	I_b	σ	ω_s	ω_Λ
$O_2\ X\ ^3\Sigma_g^-$	0	0	2	3	1
$N_2\ A\ ^3\Sigma_u^+$	1	1	2	3	1
$N_2\ B\ ^3\Pi_g$	1	1	2	3	2
$N_2^+\ X\ ^2\Sigma_g^+$	1	1	2	2	1
NO $X\ ^2\Pi$	1	0	1	2	2

C

Partition Functions

Molecule and State	Vibration-Rotation Partition Functions
$O_2\ X\ ^3\Sigma_g^-$	$Q_1(T) = \frac{0.4834\ T(1 + 0.0000149\ T)}{1 - \exp(-2256/T)}$
$N_2\ A\ ^3\Sigma_u^+$	$Q_2(T) = \frac{0.48468\ T(1 + 0.0000174\ T)}{1 - \exp(-2081.2/T)}$
$N_2\ B\ ^3\Pi_g$	$Q_3(T) = \frac{0.42670\ T(1 + 0.0000144\ T)}{1 - \exp(-2474/T)}$
$N_2^+\ X\ ^2\Sigma_g^+$	$Q_4(T) = \frac{0.3617\ T(1 + 0.0000102\ T)}{1 - \exp(-3152.5/T)}$
$NO\ X\ ^2\Pi$	$Q_5(T) = \frac{0.4098\ T(1 + 0.0000119\ T)}{1 - \exp(-2719/T)}$

Table A-2

INTENSITY FACTORS

Transition and Branch	
$^3\Pi - {}^3\Sigma$	
$R_1(J-1)$	$\dfrac{(J^2-1)\left[(J+1)u_1 - Y + 2J^2\right]^2}{(2J-1)C_1(J)}$
$Q_1(J)$	$\dfrac{\left[(J^2+J-1)u_1 + (Y-2) + 2J(J^2-1)\right]^2}{JC_1(J)}$
$Q_{R_{12}}(J-1)$	$\dfrac{(J^2-1)\left[(J+1)(Y-2) - u_1\right]^2}{JC_1(J)}$
$P_1(J+1)$	$\dfrac{J\left[J(J+2)u_1 + (J+2)(Y-2) + 2(J-1)(J+1)^2\right]^2}{(J+1)(2J+3)C_1(J)}$
$P_{Q_{12}}(J)$	$\dfrac{(2J+1)\left[(J^2+J-1)(Y-2) + u_1\right]^2}{J(J+1)C_1(J)}$
$P_{R_{13}}(J-1)$	$\dfrac{(J-1)^2(J+1)\left[(J+1)u_1 - (Y-2) - 2J(J+1)\right]^2}{J(2J-1)C_1(J)}$
$R_2(J-1)$	$\dfrac{8(J-1)(J+1)^3}{JC_2(J)}$
$R_{Q_{21}}(J)$	$\dfrac{2\left[J(Y-2) - 2\right]^2}{JC_2(J)}$
$Q_2(J)$	$\dfrac{8(2J+1)(J^2+J-1)^2}{J(J+1)C_2(J)}$
$Q_{P_{21}}(J+1)$	$\dfrac{2J\left[(J+1)Y - 2(2J+3)\right]^2}{(J+1)(2J+3)C_2(J)}$

Table A-2 (contd)

Transition and Branch	
$^3\Pi - {}^3\Sigma$	
$Q_{R_{23}}(J-1)$	$\frac{2(J+1)\left[J(Y-4)+2\right]^2}{J(2J-1)C_2(J)}$
$P_2(J+1)$	$\frac{8J^3(J+2)}{(J+1)C_2(J)}$
$P_{Q_{23}}(J)$	$\frac{2\left[(J+1)Y-2J\right]^2}{(J+1)C_2(J)}$
$R_3(J-1)$	$\frac{(J+1)\left[(J^2-1)u_3+(J-1)(Y-2)+2J^2(J+2)\right]^2}{J(2J-1)C_3(J)}$
$R_{P_{31}}(J+1)$	$\frac{J(J+2)^2\left[Ju_3-(Y-2)-2J(J+1)\right]^2}{(J+1)(2J+3)C_3(J)}$
$R_{Q_{32}}(J)$	$\frac{(2J+1)\left[(J^2+J-1)(Y-2)-u_3\right]^2}{J(J+1)C_3(J)}$
$Q_3(J)$	$\frac{\left[(J^2+J-1)u_3-(Y-2)+2J(J+1)(J+2)\right]^2}{(J+1)C_3(J)}$
$Q_{P_{32}}(J+1)$	$\frac{J(J+2)\left[J(Y-2)-u_3\right]^2}{(J+1)C_3(J)}$
$P_3(J+1)$	$\frac{J(J+2)\left[Ju_3-(Y-2)+2J(J+2)\right]^2}{(2J+3)C_3(J)}$

Table A-2 (cont'd)

Transition and Branch

where

$$u_1 = \left[Y(Y-4) + 4J^2\right]^{1/2}$$

$$u_3 = \left[Y(Y-4) + 4(J+1)^2\right]^{1/2}$$

$$C_1(J) = J(J+1)Y(Y-4) + 2(2J+1)(J-1)J(J+1)$$

$$C_2(J) = Y(Y-4) + 4J(J+1)$$

$$C_3(J) = (J-1)(J+2)Y(Y-4) + 2(2J+1)J(J+1)(J+2)$$

$^2\Sigma - {}^2\Sigma$

$P_1\ (J = K + 1/2)$	$\frac{J^2 - 1/4}{J} = \frac{2K(K+1)}{2K+1}$
$R_1\ (J = K + 1/2)$	$\frac{(J^2+1)^2 - 1/4}{J+1} = \frac{2(K+1)(K+2)}{2K+3}$
$R_{Q_{21}}(J = K + 1/2)$	$\frac{2J+1}{4J(J+1)} = \frac{2(K+1)}{(2K+1)(2K+3)}$
$P_2(J = K - 1/2)$	$\frac{J^2 - 1/4}{J} = \frac{2K(K-1)}{2K-1}$
$R_2(J = K - 1/2)$	$\frac{(J+1)^2 - 1/4}{J+1} = \frac{2K(K-1)}{2K+1}$
$P_{Q_{12}}(J = K - 1/2)$	$\frac{2J+1}{4J(J+1)} = \frac{2K}{4K^2-1}$

where

$$P_1(K + 1/2) + P_2(K - 1/2) + P_{Q_{12}}(K - 1/2) = 2K$$

$$R_1(K + 1/2) + R_2(K - 1/2) + R_{Q_{21}}(K + 1/2) = 2(K + 1)$$

Table A-2 (cont'd)

Transition and Branch $^2\Pi - {}^2\Pi$	Case "a" - Case "b"	Case "b" - Case "b"
$R_{1c}(J)$ or $R_{1d}(J)$	$\frac{J(J+2)}{J+1}$	$\frac{2K(K+2)^2}{(K+1)(2K+3)}$ where $K = J - 1/2$
$R_{2c}(J)$ or $R_{2d}(J)$		$\frac{2K^2(K+2)}{(K+1)(2K+1)}$ where $K = J + 1/2$
$Q_{1c}(J)$ or $Q_{1d}(J)$	$\frac{(2J+1)}{J(J+1)}$	$\frac{2(2K+3)}{(K+1)(2K+1)}$ where $K = J - 1/2$
$Q_{2c}(J)$ or $Q_{2d}(J)$		$\frac{2(2K-1)}{K(2K+1)}$ where $K = J + 1/2$
$P_{1c}(J)$ or $P_{1d}(J)$	$\frac{(J^2-1)}{J}$	$\frac{2(K+1)^2(K-1)}{K(2K+1)}$ where $K = J - 1/2$
$P_{2c}(J)$ or $P_{2d}(J)$		$\frac{2(K-1)^2(K+1)}{K(2K-1)}$ where $K = J + 1/2$
$P_{Q_{12c}}(J)$ or $R_{Q_{21d}}(J)$		$\frac{2(K^2-1)}{K(4K^2-1)}$ where $K = J + 1/2$
$R_{Q_{21c}}(J)$ or $R_{Q_{21d}}(J)$		$\frac{2K(K+2)}{(K+1)(2K+3)(2K+1)}$ where $K = J - 1/2$
$Q_{P_{21c}}(J)$ or $Q_{P_{21d}}(J)$		$\frac{2}{K(K+1)(2K+1)}$ where $K = J - 1/2$
$Q_{R_{12c}}(J)$ or $Q_{R_{12d}}(J)$		$\frac{2}{K(K+1)(2K+1)}$ where $K = J + 1/2$

Table A-2 (cont'd)

Transition and Branch	S_J
$^2\Sigma - {}^2\Pi$	
$R_2(J)$	$\dfrac{(2J+1)^2 \pm (2J+1)\,U(4J^2+4J+1-2Y)}{8(J+1)}$
$S_{R_{21}}(J)$	
$Q_{R_{12}}(J)$	$\dfrac{(2J+1)^2 \mp (2J+1)\,U(4J^2+4J-7+2Y)}{8(J+1)}$
$R_1(J)$	
$Q_2(J)$	$\dfrac{(2J+1)\left[(4J^2+4J-1) \pm U(8J^3+12J^2-2J+1-2Y)\right]}{8J(J+1)}$
$R_{Q_{21}}(J)$	
$P_{Q_{12}}(J)$	$\dfrac{(2J+1)\left[(4J^2+4J-1) \mp U(8J^3+12J^2-2J-7+2Y)\right]}{8J(J+1)}$
$Q_1(J)$	
$P_2(J)$	$\dfrac{(2J+1)^2 \pm (2J+1)\,U(4J^2+4J-7+2Y)}{8J}$
$Q_{P_{21}}(J)$	
$P_{12}(J)$	$\dfrac{(2J+1)^2 \mp (2J+1)\,U(4J^2+4J+1-2Y)}{8J}$
$P_1(J)$	

where

$$U = \left[Y^2 - 4Y + (2J+1)^2\right]^{-1/2}$$

Then

$$R_1(J) + {}^{R}Q_{21}(J) = \frac{2J+1}{8J}\left\{6J - 1 - U(4J^2+4J+1-2Y)\right\}$$

$$Q_1(J) + {}^{Q}P_{21}(J) = \frac{2J+1}{8(J+1)}\left\{6J + 7 + U(4J^2+4J+1-2Y)\right\}$$

$$Q_2(J) + {}^{Q}R_{12}(J) = \frac{2J+1}{8J}\left\{6J - 1 + U(4J^2+4J+1-2Y)\right\}$$

$$P_2(J) + {}^{P}Q_{12}(J) = \frac{2J+1}{8(J+1)}\left\{6J + 7 - U(4J^2+4J+1-2Y)\right\}$$

Table A-3

N2 MOLECULAR CONSTANTS

State	v	$B_v(cm^{-1})$	$D_v(10^{-6}\ cm^{-1})$	Y_v	F_{max}	$G_o(v)(cm^{-1})$
	0	1.8154	6.0	21.5	16579	0.0
$C\ ^3\Pi_u$	1	1.7932	6.0	21.5	14585	1994.2
	2	1.7682	6.0	21.4	12645	3934.4
	3	1.7407	7.5	21.1	10771.5	5808.1
	4	1.7012	11.0	20.3	8989.8	7589.8
	0	1.6285	5.8	25.9	2×10^4	0.0
$B\ ^3\Pi_g$	1	1.6108	6.0	26.2	2×10^4	1705.2
	2	1.5925	6.0	26.4	2×10^4	3381.4
	3	1.5735	6.0	26.8	2×10^4	5028.0
	4	1.5554	6.0	27.0	2×10^4	6646.6
	5	1.5364	6.0	27.3	2×10^4	8236.0
	6	1.5172	6.0	27.6	2×10^4	9796.9
	7	1.4954	6.0	27.95	2×10^4	11328.4
	8	1.4765	6.0	28.25	2×10^4	12831.0
	9	1.4576	6.0	28.5	2×10^4	14304.7
	10	1.4387	6.0	28.8	2×10^4	15749.4

Table A-3
(continued)

State	v	$B_v(cm^{-1})$	$D_v(10^{-6}\ cm^{-1})$	$G_o(v)\ (cm^{-1})$	j_{max}
$A\ ^3\Sigma_u^+$	0	1.433	5.5	0.0	100
	1	1.421	5.5	1432.5	100
	2	1.408	5.5	2837.0	100
	3	1.395	5.5	4213.3	100
	4	1.382	5.5	5561.4	100
	5	1.369	5.5	6880.9	100
	6	1.356	5.5	8171.9	100
	7	1.343	5.5	9434.1	100
	8	1.330	5.5	10667.4	100
	9	1.317	5.5	11871.7	100
	10	1.304	5.5	13046.7	100
	11	1.291	5.5	14192.4	100

Table A-4a

FRANCK-CONDON FACTORS FOR THE $A\,^3\Sigma_u^+ - B\,^3\Pi_g$ (FIRST POSITIVE) SYSTEM OF N_2

v'	v''	q	v'	v''	q
0	0	.3382	4	1	.1318
0	1	.3248	4	2	.2738
0	2	.1899	4	4	.1139
0	3	$.8857^{-1}$	4	5	.8823
1	0	.4064	4	8	$.6361^{-1}$
1	2	.1032	4	9	$.8349^{-1}$
1	3	.1782	4	10	$.7511^{-1}$
1	4	.1450	4	11	$.5510^{-1}$
1	5	$.8647^{-1}$	5	2	.2106
2	0	.1975	5	3	.1808
2	1	.2120	5	6	.1057
2	2	.1132	6	2	$.6148^{-1}$
2	4	$.7724^{-1}$	6	3	.2605
2	5	.1275	6	4	$.8305^{-1}$
2	6	.1127	6	5	.1040
2	7	$.7496^{-1}$	6	7	$.8078^{-1}$
3	0	$.5014^{-1}$	6	8	$.6967^{-1}$
3	1	.2987	7	3	.1065
3	3	.1623	7	4	.2706
3	6	$.6910^{-1}$	7	6	.1290
3	7	.1009	7	9	$.7733^{-1}$
3	8	$.9079^{-1}$	8	4	.1561
3	9	$.6406^{-1}$	8	5	.2438
			8	7	.1158

* Superscripts indicate the power of ten to which the fraction is to be raised, throughout tables.

Table A-4a (Cont'd)

v'	v''	q
9	5	.2029
9	6	.1918
9	8	$.7862^{-1}$
9	9	$.6773^{-1}$
10	5	$.5569^{-1}$
10	6	.2402
10	7	.1300
10	8	$.5219^{-1}$
10	10	$.8370^{-1}$
11	6	$.8265^{-1}$
11	7	.2630
11	8	$.7206^{-1}$
11	9	$.8779^{-1}$
11	11	$.7897^{-1}$
12	7	.1140
12	8	.2688
12	10	.1109
13	8	.1480
13	9	.2575

Table A-4b

FRANCK-CONDON FACTORS FOR $C^3\Pi_u$ - $B\ ^3\Pi_g$ (SECOND POSITIVE) SYSTEM OF N_2

v'	v''	q	v'	v''	q
0	0	.4493	2	7	$.3860^{-1}$
0	1	.3287	3	0	$.2363^{-1}$
0	2	.1469	3	1	.2515
0	3	$.5226^{-1}$	3	2	.1630
1	0	.3899	3	3	.1181
1	1	$.1868^{-1}$	3	5	$.8891^{-1}$
1	2	.2038	3	6	.1345
1	3	.2003	3	7	.1062
1	4	.1124	3	8	$.6161^{-1}$
1	5	$.4839^{-1}$	4	1	$.6957^{-1}$
2	0	.1349	4	2	.3034
2	1	.3223	4	3	$.4752^{-1}$
2	2	$.3299^{-1}$	4	4	.1570
2	3	$.5957^{-1}$	4	7	$.9955^{-1}$
2	4	.1614	4	8	.1105
2	5	.1427	4	9	$.8203^{-1}$
2	6	$.8303^{-1}$	4	10	$.4614^{-1}$

Table A-5

N_2^+ MOLECULAR CONSTANTS

State	v	$B_v(cm^{-1})$	$D_v(10^{-6}\ cm^{-1})$	F_{max}	$Go(v)\ (cm^{-1})$
$X\ ^2\Sigma_g^+$	0	1.922	6.0	19220	0.0
	1	1.902	6.0	19020	2174.8
	2	1.879	6.0	18790	4317.0
	3	1.861	6.0	18610	6426.4
	4	1.841	6.0	18410	8502.8
	5	1.826	6.0	18260	10545.8
	6	1.808	6.0	18080	12555.0
	7	1.781	6.0	17810	14530.7
	8	1.766	6.0	17660	16470.6
	9	1.740	6.0	17400	18377.6
	10	1.724	6.0	17240	20249.7
	11	1.703	6.0	17030	22086.5
	12	1.683	6.0	16830	23887.6
	13	1.663	6.0	16630	25652.4
	14	1.641	6.0	16410	27380.5
	15	1.620	6.0	16200	29071.6
	16	1.593	6.0	15930	30725.1
	17	1.572	6.0	15720	32340.5
	18	1.552	6.0	15520	33917.3
$B\ ^2\Sigma_u^+$	0	2.703	6.0	20730	0.0
	1	2.049	6.0	20490	2371.5
	2	2.025	6.0	20250	4690.3
	3	2.002	6.0	20020	6950.7
	4	1.968	6.0	19680	9147.1
	5	1.926	6.0	19260	11269.9
	6	1.896	6.0	18960	13310.9
	7	1.852	6.0	18520	15262.0
	8	1.810	6.0	18106	17100.2
	9	1.762	6.0	17620	18827.1
	10	1.710	6.0	17100	20423.8
	11	1.653	6.0	16530	21903.3
	12	1.595	6.0	15950	23275.1
	13	1.545	6.0	15450	24551.4
	14	1.494	6.0	14940	25747.7
	15	1.452	6.0	14520	26874.3
	16	1.404	6.0	14040	27941.4
	17	1.355	6.0	13550	28956.9

Table A-6

FRANCK-CONDON FACTORS FOR THE $B^2\Sigma_u^+ - X^2\Sigma_g^+$

(FIRST NEGATIVE) SYSTEM N_2^+

v'	v''	q	v'	v''	q
0	0	.6509	6	4	.2673
0	1	.2588	6	5	.2830
0	2	$.7016^{-1}$	6	6	$.5331^{-1}$
1	0	.3014	6	8	.1065
1	1	.2226	6	9	.1150
1	2	.2860	6	10	$.7442^{-1}$
1	3	.1324	6	11	$.3651^{-1}$
1	4	$.4273^{-1}$	7	4	$.2789^{-1}$
2	0	$.4537^{-1}$	7	5	.3068
2	1	.4060	7	6	.2414
2	2	$.5065^{-1}$	7	7	$.7236^{-1}$
2	3	.2290	7	9	$.8084^{-1}$
2	4	.1653	7	10	.1084
2	5	$.7113^{-1}$	7	11	$.8051^{-1}$
3	1	.1056	7	12	$.4411^{-1}$
3	2	.4137	8	5	$.3419^{-1}$
3	4	.1557	8	6	.3401
3	5	.1706	8	7	.2083
3	6	$.9451^{-1}$	8	8	$.8468^{-1}$
3	7	$.3801^{-1}$	8	10	$.5865^{-1}$
4	2	.1660	8	11	$.9821^{-1}$
4	3	.3792	8	12	$.8319^{-1}$
4	5	$.9290^{-1}$	8	13	$.5053^{-1}$
4	6	.1569	9	6	$.3890^{-1}$
4	7	.1096	9	7	.3686
4	8	$.5236^{-1}$	9	8	.1837
5	3	.2205	9	9	$.9065^{-1}$
5	4	.3310	9	11	$.4075^{-1}$
5	6	$.4815^{-1}$	9	12	$.8628^{-1}$
5	7	.1333	9	13	$.8288^{-1}$
5	8	.1161	9	14	$.5544^{-1}$
5	9	$.6488^{-1}$	10	7	$.4153^{-1}$

Table A-6 (Continued)

v'	v''	q
10	8	.3932
10	9	.1672
10	10	$.9141^{-1}$
10	13	$.7393^{-1}$
10	14	$.8018^{-1}$
10	15	$.5872^{-1}$
10	16	$.3410^{-1}$
11	8	$.4170^{-1}$
11	9	.4149
11	10	.1579
11	11	$.8818^{-1}$
11	14	$.6208^{-1}$
11	15	$.7574^{-1}$
11	16	$.6041^{-1}$
12	9	$.3928^{-1}$
12	10	.4338
12	11	.1554
12	12	$.8204^{-1}$
12	15	$.5131^{-1}$
12	16	$.7018^{-1}$
12	17	$.6066^{-1}$
12	18	$.4058^{-1}$
13	10	$.3432^{-1}$
13	11	.4496
13	12	.1593
13	13	$.7384^{-1}$
13	16	$.4189^{-1}$
13	17	$.6404^{-1}$
13	18	$.5968^{-1}$
14	12	.4614
14	13	.1697
14	14	$.6418^{-1}$
14	17	$.3390^{-1}$
14	18	$.5774^{-1}$
15	13	.4681
15	14	.1866
15	15	$.5355^{-1}$
16	14	.4676
16	15	.2104
16	16	$.4236^{-1}$
17	15	.4579
17	16	.2413

Table A-7

NO MOLECULAR CONSTANTS

State	v	B_v (cm^{-1})	D_v (cm^{-1})	Y_v	$G_1(v)$ (cm^{-1})	$G_2(v)$ (cm^{-1})
$X^2\Pi$	0	1.6957	5×10^{-6}	73.24	948.52	948.34
	1	1.6779	5×10^{-6}	74.02	2824.61	2824.08
	2	1.6601	5×10^{-6}	74.81	4672.74	4671.86
	3	1.6423	5×10^{-6}	75.62	6492.92	6491.70
	4	1.6245	5×10^{-6}	76.46	8285.13	8283.56
	5	1.6067	5×10^{-6}	77.30	10049.37	10047.44
	6	1.5889	5×10^{-6}	78.16	11785.63	11783.35
	7	1.5711	5×10^{-6}	79.05	13493.91	13491.28
	8	1.5533	5×10^{-6}	79.95	15174.18	15171.20
	9	1.5355	5×10^{-6}	80.88	16826.46	16823.13
	10	1.5177	5×10^{-6}	81.83	18450.73	18447.06
	11	1.4999	5×10^{-6}	82.80	20047.00	20042.82
	12	1.4821	5×10^{-6}	83.80	21615.13	21610.53
	13	1.4643	5×10^{-6}	84.81	23154.94	23149.82
	14	1.4465	5×10^{-6}	85.86	24666.29	24660.64
	15	1.4287	5×10^{-6}	86.93	26148.95	26142.79
	16	1.4109	5×10^{-6}	88.02	27602.67	27595.91

Table A-7 (Continued)

State	v	B_v	D_v	Y_v	$G_1(v)$	$G_2(v)$
$B^2\Pi$	0	1.118	6×10^{-6}	28.6	516.58	517.30
	1	1.105	6×10^{-6}	29	1538.66	1540.8
	2	1.093	6×10^{-6}	31	2546.4	2550.0
	3	1.081	6×10^{-6}	32	3540.4	3545.4
	4	1.068	6×10^{-6}	29	4521.2	4527.7
	5	1.056	6×10^{-6}	36	5489.4	5497.3
	6	1.041	6×10^{-6}	38	6445.6	6455.1

State	v	B_v	D_v	$G(v)$	$G_o(v)$
$A^2\Sigma^+$	0	1.9870	6×10^{-6}	1182.0	0
	1	1.9688	6×10^{-6}	3523.4	2341.4
	2	1.9498	6×10^{-6}	5833.4	4651.4
	3	1.9290	6×10^{-6}	8110.2	6928.2
	4	1.9108	6×10^{-6}	10352.6	9170.7
	5	1.8906	6×10^{-6}	12562.4	11380.4
	6	1.8684	6×10^{-6}	14740.8	13558.8
	7	1.8486	6×10^{-6}	16885.1	15703.1

Table A-8a

FRANCK-CONDON FACTORS FOR NO BETA SYSTEM ($B\ ^2\Pi - X\ ^2\Pi$)

v'	v''	q
0	5	$.5799^{-1}$
	6	.1033
	7	.1480
	8	.1735
	9	.1679
	10	.1351
	11	$.9059^{-1}$
	12	$.5068^{-1}$
1	4	$.7461^{-1}$
	5	.1103
	6	.1097
	7	$.6433^{-1}$
	10	$.5313^{-1}$
	11	.1155
	12	.1429
	13	.1233
	14	$.7983^{-1}$
2	3	$.6959^{-1}$
	4	$.9835^{-1}$
	5	$.7783^{-1}$
	9	$.8224^{-1}$
	10	$.5693^{-1}$
	13	$.7586^{-1}$
2	14	.1304
	15	.1299
	16	$.8860^{-1}$
3	2	$.5445^{-1}$
	3	$.8817^{-1}$
	4	$.7012^{-1}$
	8	$.6041^{-1}$
	11	$.5971^{-1}$
	12	$.6882^{-1}$
	15	$.6550^{-1}$
	16	.1278
4	2	$.7450^{-1}$
	3	$.7569^{-1}$
5	2	$.7975^{-1}$
	16	$.6206^{-1}$
6	1	$.6444^{-1}$
	2	$.6747^{-1}$

Table A-8b

FRANCK-CONDON FACTORS FOR NO GAMMA SYSTEM ($A\ ^2\Sigma^+ - X\ ^2\Pi$)

v'	v''	q
0	0	.1653
	1	.2636
	2	.2376
	3	.1604
	4	$.9071^{-1}$
1	0	.3291
	1	.1049
	3	$.7214^{-1}$
	4	.1349
	5	.1339
	6	$.9858^{-1}$
	7	$.6077^{-1}$
2	0	.2906
	2	.1545
	3	$.7523^{-1}$
	6	$.8848^{-1}$
	7	.1056
	8	$.8995^{-1}$
	9	$.6292^{-1}$
3	0	.1504
	1	.1903
	4	.1131
	5	$.5129^{-1}$
	8	$.6550^{-1}$
	9	$.8549^{-1}$
	10	$.7933^{-1}$
	11	$.6037^{-1}$
4	0	$.5073^{-1}$
	1	.2374
	3	.1263
	5	$.5476^{-1}$
	6	$.8784^{-1}$
	10	$.5236^{-1}$
	11	$.7116^{-1}$
	12	$.6971^{-1}$
	13	$.5636^{-1}$
5	1	.1338
	2	.1976
	4	.1026
	5	$.5125^{-1}$
	7	$.6288^{-1}$
	8	$.6791^{-1}$
	13	$.6049^{-1}$
	14	$.6148^{-1}$
6	2	.1989
	3	$.9697^{-1}$
	4	$.5754^{-1}$
	6	$.8842^{-1}$
	9	$.6284^{-1}$
	10	$.5168^{-1}$
7	2	$.9467^{-1}$
	3	.2113
	5	.1058
	7	$.7327^{-1}$
	11	$.5772^{-1}$

Table A-9

O_2 MOLECULAR CONSTANTS*

State	v	B_v (cm^{-1})	D_v ($10^{-6} cm^{-1}$)	F_{max}	$G_o(v)$ (cm^{-1})
$X\,^3\Sigma_g^-$	0	1.438	4.913	9110.5	0.0
	1	1.422	4.825	9011.8	1556.4
	2	1.406	4.737	8913.2	3089.1
	3	1.390	4.649	8814.6	4598.3
	4	1.375	4.561	8716.0	6084.4
	5	1.359	4.473	8617.3	7547.4
	6	1.343	4.385	8518.7	8987.5
	7	1.327	4.297	8420.1	10404.9
	8	1.311	4.209	8321.4	11799.7
	9	1.296	4.121	8222.8	13171.8
	10	1.280	4.033	8124.2	14521.4
	11	1.264	3.945	8025.5	15848.3
	12	1.248	3.857	7926.9	17152.7
	13	1.232	3.769	7828.3	18434.2
	14	1.217	3.681	7729.6	19693.0
	15	1.201	3.593	7631.0	20928.7
	16	1.185	3.505	7532.4	22141.2
	17	1.169	3.417	7433.8	23330.3
	18	1.154	3.329	7335.1	24495.7
	19	1.138	3.241	7236.5	25637.2
	20	1.122	3.153	7137.9	26754.4
	21	1.106	3.065	7039.2	27846.9
	22	1.090	2.977	6940.6	28914.4
	23	1.074	2.889	6842.0	29956.5
	24	1.059	2.801	6743.3	30972.6
	25	1.043	2.713	6644.7	31962.3
	26	1.027	2.625	6546.1	32925.0
	27	1.011	2.537	6447.4	33860.2
	28	0.9956	2.449	6348.8	34767.3
	29	0.9798	2.361	6250.2	35645.7

Table A-9 (Cont'd)

State	v	B_v (cm^{-1})	D_v ($10^{-6} cm^{-1}$)	F_{max}	$G_o(v)$ (cm^{-1})
$B\,^3\Sigma_u^-$	0	0.8130	4.380	7771.0	0.0
	1	0.7980	4.380	7083.0	688.0
	2	0.7850	4.380	6417.0	1353.1
	3	0.7700	4.380	5776.0	1994.6
	4	0.7540	4.380	5157.0	2612.2
	5	0.7350	4.380	4566.0	3204.0
	6	0.7190	4.380	4005.0	3765.2
	7	0.7020	4.380	3475.0	4299.2
	8	0.6710	4.380	2970.0	4799.6
	9	0.6510	4.380	2504.0	5265.0
	10	0.6330	4.380	2075.0	5694.2
	11	0.5930	4.380	1687.0	6082.4
	12	0.5625	13.000	1343.0	6427.0
	13	0.5247	16.800	1043.0	6727.9
	14	0.4836	21.200	788.0	6982.9
	15	0.4399	25.700	578.0	7192.9
	16	0.3953	34.300	409.0	7361.9
	17	0.3470	45.000	150.0	7494.8
	18	0.2960	52.00	100.00	7596.9
	19	0.2580	49.00	70.0	7672.6
	20	0.2070	76.000	35.0	7725.2

Table A-10

O_2 SCHUMANN-RUNGE FRANCK-CONDON FACTORS

v'	v''	q (v', v'')	v'	v''	q (v', v'')
0	8	$.1253^{-1}$	1	13	$.2184^{-1}$
0	9	$.2802^{-1}$	1	15	$.1833^{-1}$
0	10	$.5326^{-1}$	1	16	$.6708^{-1}$
0	11	$.8667^{-1}$	1	17	.1137
0	12	.1213	1	18	.1301
0	13	.1465	1	19	.1120
0	14	.1528	2	2	$.6472^{-4}$
0	15	.1379	2	3	$.4520^{-3}$
0	16	.1074	2	4	$.2200^{-2}$
0	17	$.7210^{-1}$	2	5	$.7886^{-2}$
0	18	$.4159^{-1}$	2	6	$.2138^{-1}$
0	19	$.2051^{-1}$	2	7	$.4420^{-1}$
1	2	$.1294^{-9}$	2	8	$.6899^{-1}$
1	3	$.1022^{-3}$	2	9	$.7819^{-1}$
1	5	$.2407^{-2}$	2	10	$.5804^{-1}$
1	6	$.7886^{-2}$	2	11	$.2000^{-1}$
1	7	$.2049^{-1}$	2	13	$.2139^{-1}$
1	8	$.4262^{-1}$	2	14	$.6073^{-1}$
1	9	$.7084^{-1}$	2	15	$.6959^{-1}$
1	10	$.9271^{-1}$	2	16	$.3556^{-1}$
1	11	$.9195^{-1}$	2	18	$.1536^{-1}$
1	12	$.6286^{-1}$	2	19	$.7004^{-1}$

Table A-10 (Continued)

v'	v''	q (v', v'')	v'	v''	q (v', v'')
3	0	$.1043^{-5}$	4	6	$.5306^{-1}$
3	1	$.2243^{-4}$	4	7	$.6118^{-1}$
3	2	$.2248^{-3}$	4	8	$.3937^{-1}$
3	3	$.1386^{-2}$	4	11	$.3550^{-1}$
3	4	$.5844^{-2}$	4	12	$.4551^{-1}$
3	5	$.1767^{-1}$	4	13	$.1519^{-1}$
3	6	$.3896^{-1}$	4	15	$.3357^{-1}$
3	7	$.6189^{-1}$	4	16	$.4976^{-1}$
3	8	$.6716^{-1}$	4	17	$.1687^{-1}$
3	9	$.4256^{-1}$	4	19	$.4176^{-1}$
3	12	$.3544^{-1}$	5	1	$.1711^{-3}$
3	13	$.5616^{-1}$	5	2	$.1374^{-2}$
3	14	$.3187^{-1}$	5	3	$.6558^{-2}$
3	16	$.1776^{-1}$	5	4	$.2038^{-1}$
3	17	$.5938^{-1}$	5	5	$.4224^{-1}$
3	18	$.5971^{-1}$	5	6	$.5654^{-1}$
3	19	$.1770^{-1}$	5	7	$.4268^{-1}$
4	0	$.3479^{-5}$	5	8	$.1022^{-1}$
4	1	$.6790^{-4}$	5	10	$.2965^{-1}$
4	2	$.6084^{-3}$	5	11	$.4003^{-1}$
4	3	$.3310^{-2}$	5	12	$.1149^{-1}$
4	4	$.1202^{-1}$	5	14	$.3425^{-1}$
4	5	$.3033^{-1}$	5	15	$.3611^{-1}$

Table A-10 (Continued)

v'	v''	q (v', v'')	v'	v''	q (v', v'')
5	16	$.3720^{-1}$	7	4	$.3759^{-1}$
5	17	$.1360^{-1}$	7	5	$.4900^{-1}$
5	18	$.4761^{-1}$	7	6	$.3094^{-1}$
5	19	$.2836^{-1}$	7	9	$.3321^{-1}$
6	1	$.3736^{-3}$	7	10	$.2094^{-1}$
6	2	$.2683^{-2}$	7	12	$.2098^{-1}$
6	3	$.1121^{-1}$	7	13	$.3004^{-1}$
6	4	$.2956^{-1}$	7	15	$.1305^{-1}$
6	5	$.4930^{-1}$	7	16	$.3437^{-1}$
6	6	$.4767^{-1}$	7	17	$.8005^{-2}$
6	7	$.1874^{-1}$	7	18	$.8607^{-2}$
6	9	$.2025^{-1}$	7	19	$.3852^{-1}$
6	10	$.3754^{-1}$	8	2	$.7343^{-2}$
6	11	$.1415^{-1}$	8	3	$.2323^{-1}$
6	13	$.2919^{-1}$	8	4	$.4259^{-1}$
6	14	$.3050^{-1}$	8	5	$.4158^{-1}$
6	16	$.1677^{-1}$	8	6	$.1390^{-1}$
6	17	$.4002^{-1}$	8	8	$.2307^{-1}$
6	18	$.1169^{-1}$	8	9	$.2829^{-1}$
6	19	$.6046^{-2}$	8	11	$.1033^{-1}$
7	1	$.7262^{-3}$	8	12	$.2975^{-1}$
7	2	$.4660^{-2}$	8	15	$.3032^{-1}$
7	3	$.1698^{-1}$	8	16	$.1014^{-1}$

Table A-10 (Continued)

v'	v''	q (v', v'')
8	17	$.5726^{-1}$
8	18	$.3281^{-1}$
8	19	$.1098^{-1}$
9	2	$.1065^{-1}$
9	3	$.2910^{-1}$
9	4	$.4341^{-1}$
9	5	$.2967^{-1}$
9	8	$.2931^{-1}$
9	9	$.1313^{-1}$
9	11	$.2422^{-1}$
9	12	$.1651^{-1}$
9	14	$.2382^{-1}$
9	15	$.1607^{-1}$
9	16	$.1294^{-2}$
9	17	$.2692^{-1}$
9	18	$.1339^{-1}$
10	2	$.1439^{-1}$
10	3	$.3372^{-1}$
10	4	$.4000^{-1}$
10	5	$.1701^{-1}$
10	7	$.1903^{-1}$
10	8	$.2433^{-1}$
10	10	$.1193^{-1}$
10	11	$.2386^{-1}$
10	13	$.1271^{-1}$
10	14	$.2247^{-1}$
10	16	$.1795^{-1}$
10	17	$.1902^{-1}$
11	3	$.3645^{-1}$
11	4	$.3327^{-1}$
11	5	$.6897^{-2}$
11	7	$.2481^{-1}$
11	8	$.1333^{-1}$
11	10	$.2122^{-1}$
11	11	$.1208^{-1}$
11	13	$.2231^{-1}$
11	16	$.2304^{-1}$
12	3	$.3695^{-1}$
12	4	$.2477^{-1}$
12	6	$.1126^{-1}$
12	7	$.2375^{-1}$
12	10	$.2114^{-1}$
12	12	$.1175^{-1}$
12	13	$.1758^{-1}$
12	15	$.1868^{-1}$
13	3	$.3526^{-1}$

Table A-10 (Continued)

v'	v''	q (v', v'')	v'	v''	q (v', v'')
13	4	$.1616^{-1}$	16	5	$.1140^{-1}$
13	6	$.1764^{-1}$	16	6	$.1694^{-1}$
13	7	$.1750^{-1}$	16	8	$.1274^{-1}$
13	9	$.1582^{-1}$	16	9	$.1062^{-1}$
13	10	$.1339^{-1}$	16	11	$.1597^{-1}$
13	12	$.1878^{-1}$	16	14	$.1066^{-1}$
13	15	$.1854^{-1}$	17	5	$.1484^{-1}$
14	4	$.3176^{-1}$	17	6	$.1199^{-1}$
14	4	$.8805^{-2}$	17	8	$.1536^{-1}$
14	6	$.2089^{-1}$	17	11	$.1330^{-1}$
14	7	$.9600^{-2}$	17	13	$.1393^{-1}$
14	9	$.1898^{-1}$	18	5	$.1661^{-1}$
14	12	$.1685^{-1}$	18	8	$.1491^{-1}$
14	14	$.1528^{-1}$	18	13	$.1328^{-1}$
15	6	$.2040^{-1}$	19	5	$.1661^{-1}$
15	9	$.1649^{-1}$	19	8	$.1210^{-1}$
15	11	$.1358^{-1}$	20	5	$.1515^{-1}$
15	14	$.1673^{-1}$			

Appendix B

SUPPLEMENTARY NUCLEAR WEAPON EFFECTS STUDY

B.1 INTRODUCTION

The proper theoretical description of the fireball resulting from a nuclear detonation requires that the radiative transport of energy be included in the appropriate hydrodynamical description of the fireball development. When this is attempted, it is quickly found that numerical calculations are required to solve the equations involved. The machine codes for such numerical computations are commonly referred to as coupled radiation-hydrodynamics codes.

Brode (Ref. 23), of the Rand Corporation, has used such codes for a variety of fireball computations. His results are valid at earlier times when the fireball is essentially optically thick and when the energy lost is small compared to the internal energy of the system. In terms of low altitude fireball phenomenology, his results are valid at times earlier than the time to light minimum. It is to be noted that the fireball is still optically thick at this time, and only a small fraction of the weapon yield has escaped the system via thermal radiation. It should further be noted that the time of minimum corresponds approximately to the time at which the shock wave departs from the radiating region of the fireball, and the Brode results should thus give an adequate description of the advancing shock front.

Proper theoretical description of the final pulse of thermal radiation, which involves as much as half of the weapon yield, requires that the radiation-hydrodynamics code be capable of treating radiative transport in both optically thick and optically thin media in conjunction with the appropriate hydrodynamics. Such a code has been developed and is described below.

B.2 GENERAL DESCRIPTION

The code developed for late time fireball computations is a generalization of the Richtmyer-von Neumann artificial viscosity technique for a spherical Lagrangian system in which the divergence of the radiative flux appears in the hyperbolic partial differential equation which expresses the conservation of energy for a given mass zone. The basic differential equations are those given by Richtmyer (Ref. 24)

$$\frac{\partial U}{\partial t} = -\frac{1}{\rho_o}\left[\frac{R(r,t)}{r}\right]^2 \frac{\partial p}{\partial r} \qquad (B.1)$$

$$\frac{\partial R}{\partial t} = U \qquad (B.2)$$

$$\frac{\partial \epsilon}{\partial t} = \frac{P}{\rho^2}\frac{\partial \rho}{\partial t} + \frac{1}{\rho}\nabla \cdot F \qquad (B.3)$$

modified to include this additional radiative term. Without this term, the solution of the equations is a standard initial value problem which can be integrated explicitly. Such solutions are well known; only those modifications required to include the radiative transport will be discussed here.

Formulation of the Radiative Energy Transport

To understand the basic problem of radiative transport, consider the standard equation of radiative transfer for a medium in local thermodynamic equilibrium and for a plane parallel geometry:

$$\cos\theta \frac{dI_\nu(x,\cos\theta)}{\rho dx} = \kappa_\nu \left\{B_\nu\left[T(x)\right] - I_\nu(x\cos\theta)\right\} \qquad (B.4)$$

where the quantities are defined in the standard terminology as given by Chandrasekhar (Ref. 25).

This equation represents the change in the specific intensity of the radiation along a ray having a given direction in space. Since an infinite number of directions for rays can be assigned to any unit volume under consideration, it is clear that Eq. (B.4) represents an infinite set of differential equations which are functions of position, direction in space, and radiation frequency.

The solution for this set of equations has been obtained in closed form by Chandrasekhar (Ref. 25, p. 55 ff) based on a method in which the radiation field is represented by $2N$ streams where, in the limit, N approaches infinity. The convergence of this solution is shown to be critically dependent on the proper choice of radiation streams used in the first approximation, i.e., $N = 1$, which corresponds to the two-stream method of A. Schuster and K. Schwarzschild (1905). Suitable choice of the directions of the two rays used to represent the radiation field results in a formulation of the gross energy transport, whose accuracy is considerably greater than the accuracy with which we know the appropriate absorption coefficients. The accuracy of this approach improves when it is applied to thin isothermal slabs as contrasted with the usual application to an atmosphere of essentially infinite extent.

The basic physics of the Schuster-Schwarzschild method has been carried over to spherical geometry. In this application, the inclination of the chosen radiation streams changes with the relative radius of curvature of the spherical zones. When the radius of curvature becomes large compared to the zone thickness, the appropriate inclination is that which is applicable for plane-parallel geometry. Indeed, in this limit, the exact solution for the flux in terms of exponential integrals may be employed and no approximation is required. However, in the present application, other conditions of the problem made it desirable to maintain the two-stream approximation, the choice of inclination being determined by the condition that the difference in these two solutions be held to a minimum. The proper choice of inclination near the center of the sphere has been temporarily postponed by choosing the central zones such that they are optically thick and by requiring that the two-stream solution transform into the diffusion approximation which is applicable under these conditions.

The actual formulation of the flux is then carried out using the formal integral solution (Ref. 25) of the equation of transfer for the specific intensity along the representative rays. The source function is assumed to be that which is appropriate under conditions of local thermodynamic equilibrium and is expanded in terms of the temperatures – and derivatives of the temperatures – at the zone boundaries. While the code has been written to allow the spectrum to be divided into any desired number of frequency bands, the initial computations have been carried out using the Rosseland mean absorption coefficients for the purposes to be enumerated later.

The numerical solution is carried out by explicit integration of the basic equations, except for the energy equation, using the well-known Richtmyer-von Neumann method (Ref. 26). The integration of the energy equation cannot be carried out explicitly since the radiative flux term for any particular zone is dependent upon the temperatures of the neighboring zones. Since the density is known at this stage of the solution, it is convenient to express the energy equation in terms of zone temperatures alone. The solution is then carried out by assuming an approximate temperature for each zone and using a Newton-Raphson iteration scheme to adjust the zone temperatures until changes in temperatures on subsequent iterations are less than a pre-determined amount.

This method of iteration involves the solution of N linear equations in N unknowns, where N is the number of zones and is usually of the order of a hundred. Such a system is in principle easily soluble by computer methods, but the procedure is time consuming. In practice only a few zones in each direction measurably influence the temperature iteration for a particular zone, which results in a simplification. In a first solution of the problem a five-zone centered system has been used which results in a matrix having five terms across the diagonal. After suitable scaling, such a system is rapidly soluble by direct elimination and back substitution.

As part of the check out procedure, the equation of state and formulation of the mean absorption coefficient given by Brode (Ref. 23) were used so as to reproduce his results over an appropriate period of fireball history. Using 100 zones, and 3 iterations per

hydrodynamical cycle, the code proceeds successfully about 200 time steps per hour. With minor modifications, the code has also been applied to a problem in thermal ablation in fireballs and to problems in stellar stability.

Interpolation formulae are currently being written for mean absorption coefficients for chosen spectral bands appropriate to late fireball development.

Initial Energy Deposition in Variable Density Atmosphere

When a nuclear device is detonated in the atmosphere, a large percentage of the energy released is radiated away and is deposited in the surrounding atmosphere. Since the air density exhibits a large variation with altitude, it follows that the scale of distances over which this energy is absorbed by the air will be dpendent upon the burst altitude. Consequently the energy density also exhibits a dependence on altitude.

The sequence of radiative and hydrodynamic events which follows this initial phase is dependent upon the radial energy distribution. Thus, one would expect the scaling laws, for various weapons effects as a function of altitude, to also exhibit a dependence on the initial energy deposit. It is therefore of interest to perform computations of this distribution as a function of weapon yield and altitude.

Because of the large number of cases of interest, a machine code was written to perform the appropriate computations. The basic equations involved are

$$\frac{dE}{dR} = \frac{1}{4\pi R^2} \int W_\nu \, \kappa(\rho,\nu) \, \rho(A) \, e^{-\int_0^R \kappa(\rho,\nu)\,\rho(A)\,dR} \, d\nu \qquad \text{(B.5)}$$

$$\rho = \rho(A) \qquad \text{(B.6)}$$

$$\kappa_\nu = \kappa(\rho, \nu) \tag{B.7}$$

$$\bar{T} = \bar{T}(\bar{E}, \rho) \tag{B.8}$$

where

$\frac{d\bar{E}}{d\bar{R}}$ = energy per unit volume deposited at a distance $\bar{R}$ from the point of detonation.

ρ = air density as a function of altitude A

κ_ν = absorption coefficient of air

W_ν = total energy of frequency ν radiated by the source.

Equation (B.6) was evaluated by using an empirical fit to the ARDC Standard Atmosphere (Ref. 27).

The absorption coefficients used were those of Gilmore (Ref. 28) for cold air. Stripping was neglected since it appears to have only a small effect upon the later development.

In coding the problem, the radiative output of the source was divided into 11 separate spectral regions, and a corresponding average opacity was chosen for each of these regions. A minor modification of the code allows a larger number of spectral regions to be used when desired. The code carries out radial computations for the downward direction and at directions in space differing by 10 deg, or any multiple of 10 deg, as may be desired. The printed output for each direction in space lists the radius from the point of detonation for 35 different points and the air density, altitude, and energy density for each point.

Temperatures were determined using the tabulated equation-of-state data given by Gilmore (Ref. 16), and Hilsenrath and Beckett (Ref. 29). Initial runs have shown that a better representation of the equation of state for air is desirable.

The initial runs included a variety of yields and altitudes, including cases applicable to previous field test situations and cases of interest for future planning. Considerable success was obtained in predicting a number of the effects observed in earlier field tests, but a better handling of the equation of state is indicated before the results are presented in scaling law form.